

# Calorimetric Determination of Energy Levels in Rare-Earth and Yttrium-Iron Garnets

A. BROOKS HARRIS AND HORST MEYER\*

*Gordon McKay Laboratory, Harvard University, Cambridge, Massachusetts,  
and Department of Physics, Duke University, Durham, North Carolina*

(Received February 26, 1962)

It is shown that low-temperature calorimetry can be a sensitive method for determining the lowest excited energy levels in the rare-earth iron garnets. From Pauthenet's magnetization data one expects the lowest excited levels of several rare-earth ions to become populated at temperatures well below 20°K and to contribute a large specific heat. This property offers the possibility of testing the validity of the Weiss molecular field and spin-wave approximations for this isomorphic series of oxides. After a discussion of the specific heat in terms of the Weiss molecular-field approximation, a spin-wave treatment for the garnets is then presented and the dispersion equation for the acoustical branch is derived. It is shown by a perturbation calculation that in garnets with magnetic rare-earth ions, there are twelve low-lying optical modes that will contribute to the specific heat below 20°K. Heat-capacity measurements between 1.3 and 20.6°K on the iron garnets of Y, Sm, Gd, Tb, Dy, Ho, Er, Yb, and Lu are presented and interpreted in terms of the two theoretical models. The energy levels so obtained are compared to those measured by optical

absorption and deduced from magnetic data. For YIG and LuIG, where only the acoustical mode contributes to the magnetic specific heat, the result is compared to other heat-capacity and magnetic measurements. With the exception of TbIG and SmIG the magnetic specific heat of the garnets can be satisfactorily interpreted. Reasonable agreement is obtained in particular between the energy levels as deduced from specific heat data and those observed directly by optical absorption on YbIG and ErIG. In general it is found that for temperatures lower than  $\sim E_1/2k_B$ , where  $E_1$  is the energy of the lowest excited level and  $k_B$  the Boltzmann constant, the spin-wave approximation can be used to interpret the results, while for temperatures larger than about  $E_1/6k_B$  the Weiss molecular-field treatment is valid. In the overlapping temperature range, both approximations are equally good. The nuclear magnetic specific heat for TbIG and HoIG is observed and is found to be consistent with the predictions from resonance measurements in other rare-earth compounds.

## I. INTRODUCTION

THE series of the rare-earth iron garnets is probably the most thoroughly investigated one of all ferrites, because of several properties which make the experimental and theoretical studies very rewarding. By substituting the various rare-earth ions into the garnet lattice one can study the effects of these ions on the macroscopic properties. Also, within the iron garnets there are a variety of magnetic interactions, which provide a detailed test for any proposed theoretical model. Finally, the fact that all the crystallographic sites are occupied and all the iron ions are trivalent (unlike in the spinels) accounts for a great chemical stability of the garnets and a good reproducibility of their physical properties.

The compounds, so named because they are isostructural with the naturally occurring garnets, almandine and grossularite, have the chemical formula  $5\text{Fe}_2\text{O}_3 \cdot 3M_2\text{O}_3$  and are usually denoted MIG, where  $M$  is either a trivalent yttrium ion or rare-earth ion from samarium to lutetium. The rare-earth ions preceding samarium in the periodic table are too large to fit into the garnet lattice except in small concentrations. The unit cell, which has cubic symmetry,<sup>1</sup> contains four formula units of garnet whose positive ions are distributed over 3 types of sites. The ferric ions occupy the 16  $a$  sites at the center of a tetrahedron of oxygen ions and the 24  $d$  sites at the center of an octahedron of oxygen ions. The  $M^{3+}$  ions occupy the 24  $c$  sites at the center of a distorted cube of oxygen ions. Not all the sites of a given type are crystallographically equivalent. For instance there are six inequivalent  $c$  sites

From Pauthenet's<sup>2</sup> and Aléonard's<sup>3</sup> magnetic measurements, an adequate picture of the interactions between the magnetic ions could be obtained in the way indicated by Néel<sup>4</sup>: the ferric ions on the  $a$  sites are strongly coupled antiferromagnetically to those of the  $d$  sites. The resultant magnetization of these two sublattices is in turn antiferromagnetically coupled to the spins of the ions on the  $c$  sites, this interaction being an order of magnitude smaller than the first one. The coupling between the  $a$  and  $d$  sublattices is responsible for the Curie point at about 550°K, which is approximately the same for all the iron garnets. Below 70°K, when the iron ions on the  $a$  and  $d$  sublattices are nearly aligned, the effective Weiss molecular field acting on the iron ions is of the order of  $5 \times 10^6$  G. In contrast, the field acting on the ions of the  $c$  sublattice is of the order of  $2 \times 10^5$  G which produces energy level splittings of the order of 20–50  $\text{cm}^{-1}$ .

The magnetic ions are also subjected to a crystalline electric field, which in general is different for crystallographically inequivalent sites. For  $S$ -state ions the effect of the crystalline field is negligible in comparison to that of the exchange field. As a result, it is often unnecessary to distinguish between the inequivalent  $a$  or  $d$  or even  $c$  sites when the  $M$  ion is in an  $S$  state. When the  $M$  ion is not in an  $S$  state, the crystalline field splittings are of the same order as the exchange splittings, sometimes even much larger, as for YbIG.<sup>5</sup> Therefore the magnetic moment of each level will be rather different from that of the free ion, and in general

<sup>2</sup> R. Pauthenet, *Ann. phys.* **3**, 424 (1958); *J. phys. radium* **20**, 388 (1959).

<sup>3</sup> R. Aléonard, *J. Phys. Chem. Solids* **15**, 167 (1960).

<sup>4</sup> L. Néel, *Ann. phys.* **3**, 137 (1948).

<sup>5</sup> R. Pappalardo and D. L. Wood, *J. Chem. Phys.* **33**, 1734 (1960).

\* Alfred P. Sloan Fellow.

<sup>1</sup> R. Wyckoff, *Crystal Structures* (Interscience Publishers, Inc., New York, 1953), Vol. III, Chap. 12.

anisotropic. This results in a large anisotropy field, and it turns out that at low enough temperatures the effective field in an unmagnetized sample lies along a [111] direction in the unit cell. Under these conditions the number of effectively inequivalent  $c$  sites is reduced to two, and one expects different splittings for each.

It is always of great interest to determine the energy levels and the eigenfunctions of these magnetic ions and to verify how well the macroscopic properties can be deduced from them. This goal, however, is rendered very difficult by the complexity of the garnet crystal and by the many unknown parameters such as the crystalline fields. As a part of the effort to obtain information on the energy levels in the iron garnets, we have measured the specific heat of the garnets of Y, Sm, Gd, Tb, Dy, Ho, Er, Yb, and Lu between 1.3 and 20.6°K. The rare earth garnets are indeed a very favorable system for such an investigation, as can be seen by a simple estimation: the levels of  $M^{3+}$  split by the exchange field will be appreciably populated at temperatures above say 4°K and will give a large contribution to the heat capacity, proportional to

$$(E_1/k_B T)^2 \exp(-E_1/k_B T) \quad \text{for } (E_1 \gg k_B T),$$

where  $E_1$  is the energy of the first excited level and  $k_B$  is the Boltzmann constant. On the other hand one can estimate that the lattice specific heat should be relatively small up to 20°K and it can be measured well enough on a garnet such as YIG and LuIG, where this large "magnetic" specific heat is absent. The splitting hence can be determined to an accuracy often better than 5% and in favorable cases the position of the next excited level can also be determined, although with less accuracy than the first. If too many levels are clustered close together, the calorimetric method is only able to give an average splitting. Eventually the most accurate value of the energy levels for all the garnets will be obtained from optical absorption experiments. It should be pointed out here that in such absorption methods one usually measures transitions between levels at  $\mathbf{k}=0$  in the spin wave spectrum ( $\mathbf{k}$  being the wave vector) while the macroscopic properties such as specific heat and magnetization are determined by the average over the  $\mathbf{k}$  values for each branch of the spectrum. Hence it should not be surprising to find in some cases discrepancies between calorimetric and optical measurements at temperatures where the spin wave approximation is expected to hold. So far, satisfactory agreement between calorimetric and optical<sup>6</sup> experiments have been obtained for YbIG and ErIG.

One is interested to know over what temperature range the thermal and magnetic properties of these garnets can be accounted for by the Weiss molecular field (henceforth denoted WMF) and the spin-wave approximations. Accordingly we have carried out calculations determining the low-frequency spin-wave

modes and we have compared our prediction with experiment. It will be shown that for  $k_B T \lesssim E_1/6$ , where  $E_1$  is the lowest exchange splitting, the spin-wave approximation gives the best results, as one would expect. At higher temperatures, the one-ion picture of the WMF model fits the results remarkably well.

In addition, specific heat measurements can give information on the nuclear energy levels. Here again, such a determination is obviously not as accurate as a direct spectroscopic measurement, but it can give a good idea of the frequency at which resonance should be observed. A direct determination of the nuclear energy levels in the garnets has not been carried out so far.

## II. EXPERIMENTAL

### A. Apparatus

In order to carry out the proposed measurements, we have constructed a cryostat of the type described by Hill<sup>7</sup> and by Smith and Wolcott,<sup>8</sup> to be operated between 1.3 and 21°K. Some of the measurements, including those on samples with a small specific heat (YIG and LuIG), were carried out in another calorimeter in which the sample could be brought in contact with the low-temperature bath by means of a simple heat switch. The temperature was measured by a 68- $\Omega$ ,  $\frac{1}{16}$ -W Allen Bradley carbon resistor which was calibrated between 1.3 and 4.2°K and between 13 and 20.6°K against the vapor pressure of helium and normal hydrogen ( $\frac{1}{4}$  para,  $\frac{3}{4}$  ortho), respectively. Between 4 and 13°K, the carbon thermometer was calibrated against a helium gas thermometer.

As a test of the apparatus and of the various calibrations, we have measured the heat capacity of a 150-g cylinder of copper with a purity of 99.99%. The results so obtained agreed well with the data of Corak *et al.*<sup>9</sup> between 1.3 and 4.2°K and with those of Kok and Keesom,<sup>10</sup> and Giauque and Meads<sup>11</sup> above 4°K and will be reported elsewhere.

At the beginning of this work, it was feared that the thermal diffusivity inside the sample would be small enough to cause thermal lags during the heat capacity measurements. Accordingly the calorimeter consisted of a thin-walled copper container filled with small garnet slugs of about 2 g each and a very small amount of helium exchange gas. Later, the samples consisted of a cylinder of garnet material to which the heater and the carbon resistor were directly attached. After each heating period, thermal equilibrium was usually achieved in less than a minute.

<sup>7</sup> R. W. Hill, J. Sci. Instr. **30**, 331 (1953).

<sup>8</sup> P. L. Smith and N. Wolcott, Phil. Mag. **1**, 854 (1956).

<sup>9</sup> W. S. Corak, M. P. Garfunkel, C. B. Satterthwaite, and A. Wexler, Phys. Rev. **98**, 1699 (1955).

<sup>10</sup> J. A. Kok and W. H. Keesom, Physica **3**, 1035 (1936).

<sup>11</sup> W. F. Giauque and P. F. Meads, J. Am. Chem. Soc. **63**, 1897 (1941).

<sup>6</sup> M. Tinkham, J. Appl. Phys. **33**, 1248S (1962).

### B. The Samples

All the samples were polycrystalline and with the exception of YIG and SmIG were prepared at the Gordon McKay Laboratory using the coprecipitation method described by Wolf and Rodrigue.<sup>12</sup> The original reagents had a purity of at least 99.99%. It is possible that the sample could be slightly contaminated during the preparation, but this will not affect the specific heat results unless the impurity has a much larger heat capacity per unit volume than the sample. For this reason it was important that YIG and LuIG should contain as little rare-earth impurity as possible. We estimated that the effect of the impurity on the specific heat was less than 2% in this case and was negligible for the other rare-earth garnets.

More important however was the possibility of the presence of  $M_2O_3$ ,  $Fe_2O_3$ , and  $MFeO_3$  which had not reacted. An upper limit for the concentration of these oxides could be established by analysis of x-ray pattern. Since the position of the characteristic line of  $MFeO_3$  was known, it was possible to check for its presence in the garnet. Except for the LuIG sample, the orthoferrite line was missing in the x-ray spectrum and therefore the  $MFeO_3$  concentration was estimated to be less than 4%. This should not affect the lattice specific heat appreciably because the elastic constants and hence  $\Theta_D$  are expected to be about the same for all the oxides. However, the presence of oxides may cause a slight error in the magnetic specific heat.

Unfortunately polycrystalline samples are porous to a certain extent. In order to estimate the porosity, the density was measured by the gravitation method and compared to that obtained from x rays. This comparison is given in Table I together with the respective masses of the specimens. No systematic studies of the effect of porosity on the lattice specific heat have been carried out. However, a simple argument based on the phonon spectrum in relation to the grain size shows that the specific heat should not be influenced by porosity at temperatures above 0.1°K.

The ceramic sample of SmIG obtained from Microwave Chemical Associates was more intensively analyzed due to the unusual specific heat results it gave at temperatures below 5°K. An x-ray fluorescence analysis, kindly performed by Professor Frondel of the Mineralogy Department at Harvard University verified that the chemicals used in the fabrication of the sample were pure. By inspection of a polished surface under an electron microscope, Professor Frondel was able to find about 2% impurity, no doubt an oxide of the type mentioned before. Probably all the samples had this kind of impurity so it is strange that only SmIG should give unexpected results.

The YIG sample was prepared from especially pure materials by Dr. J. E. Kunzler at Bell Telephone Laboratories. It consisted of two cylinders of about

TABLE I. Density and mass of the garnet samples.

<i>M</i>	$\rho$ (x rays) (g/cc)	$\rho$ (average) (g/cc)	Mass of sample (g)
Y	5.17	5.10	90.70
Sm	6.27	6.07	199.03
Gd	6.46	6.22	71.61
Tb	6.52	6.16	111.75
Dy	6.67	6.52	78.85
Ho	6.76	5.97	82.97
Er	6.84	6.00	80.91
Yb	7.08	6.95	93.63
Lu	7.16	7.03	70.28

1.5-cm diam and 1-cm length which were glued together with a small amount of G.E. varnish.

### III. THEORETICAL SURVEY

#### A. Lattice Specific Heat

For magnetic insulators such as the garnets, the Hamiltonian of the system can be written in first approximation as

$$\mathcal{H} = \mathcal{H}_{\text{latt}} + \mathcal{H}_{\text{magn}} + \mathcal{H}_{\text{nuc1}}, \quad (1)$$

where  $\mathcal{H}_{\text{latt}}$  depends only on the nuclear position and momentum coordinates,  $\mathcal{H}_{\text{magn}}$  describes the behavior of the unpaired (magnetic) electrons, and  $\mathcal{H}_{\text{nuc1}}$  describes the interaction of the nuclear spins with the electron spins. It can be shown that to a sufficient accuracy the specific heat resulting from the Hamiltonian (1) is given by

$$C = C_{\text{latt}} + C_{\text{magn}} + C_{\text{nuc1}}, \quad (2)$$

where each term on the right side arises from the corresponding one in Eq. (1). In order to determine  $C_{\text{magn}} + C_{\text{nuc1}}$  from the total specific heat, one must know  $C_{\text{latt}}$ , which in most cases cannot be determined directly. We assumed therefore that  $C_{\text{latt}}$  of the rare earth garnets could be taken to be approximately that of LuIG, which has been measured accurately (See Sec. IV A1.). Hence

$$C_{\text{magn}} + C_{\text{nuc1}} = C - C_{\text{latt}}(\text{LuIG}). \quad (3)$$

This assumption did not introduce serious errors in the determination of the magnetic specific heat which was the dominant term for the other rare earth garnets up to 20°K. For YIG, on the other hand, the lattice specific heat will be somewhat different, mainly because of the large difference in molecular weight. It can be shown that at low temperatures the Debye  $\Theta$  is proportional to  $(\bar{m})^{-1/3}$ , where  $\bar{m}$  is an average mass of the atoms in the unit cell which can be calculated exactly only if the normal modes of vibration of the lattice are known. If one assumes in first approximation that  $\bar{m}$  is proportional to the molecular weight,  $\Theta(\text{YIG})$  should be 15% larger than  $\Theta(\text{LuIG})$ .

<sup>12</sup> W. P. Wolf and G. P. Rodrigue, J. Appl. Phys. **29**, 105 (1958).

### B. Magnetic Specific Heat Derived from the One-Ion Approximation

Assuming the validity of Hund's rule, we have:

$$\mathcal{H}_{\text{magn}} = \mathcal{H}_{\text{s.o.}} + V_{\text{crystal}} + \mathcal{H}_{\text{ex}} + \mathcal{H}_{\text{dip}}, \quad (4)$$

where  $\mathcal{H}_{\text{s.o.}}$  is the spin-orbit interaction  $AL \cdot S$ ,  $V_{\text{crystal}}$  is the crystalline electric field potential,  $\mathcal{H}_{\text{ex}}$  is the exchange Hamiltonian, and  $\mathcal{H}_{\text{dip}}$  is the dipolar interaction. Usually one writes

$$\mathcal{H}_{\text{ex}} = -2 \sum_{\text{pairs}} J_{ij} \mathbf{S}_i \cdot \mathbf{S}_j, \quad (5)$$

where  $J_{ij}$  is the exchange integral between the ions  $i$  and  $j$  and in most cases only the nearest neighbors are considered.

In the WMF approximation, the individual interactions are replaced by effective fields  $H_{\text{eff}}^i$  acting on the ion  $i$  in a self-consistent manner, and which are linearly related to the magnetic moments of the various sublattices. For the particular case of the iron garnets, let us use the notation of Pauthenet<sup>2</sup> and Aléonard<sup>3</sup> in the *Journal de physique et le radium*. There one has

$$H_{\text{eff}}^i = \sum_j n_{ij} M_j, \quad (6)$$

where  $M_j$  is the magnetic moment of the  $j$  sublattice per mole of garnet and  $n_{ij}$  is a coupling constant related to the exchange integral by the equation<sup>13</sup>

$$n_{ij} = \left( \frac{J_{ij}}{k_B} \right) \frac{(g_i - 1)(g_j - 1)}{g_i g_j} \frac{z_{ij}}{3.00[j]}. \quad (7)$$

Here  $z_{ij}$  is the number of ions  $j$  surrounding an ion  $i$ ,  $g_i$  and  $g_j$  are the Landé factors for the corresponding ions and  $[j]$  is the relative concentration of  $j$  sites. As shown by magnetic measurements, the components of this symmetric matrix  $n$  are such that

$$n_{aa}, n_{ad}, n_{dd} \gg n_{dc}, n_{ac} \gg n_{cc}. \quad (8)$$

Hence we neglect the effect of the  $M^{3+}$  ions on the  $a$  and  $d$  sublattices and on each other. At temperatures below 20°K, the magnetic moments of sublattices  $a$  and  $d$  have practically reached their saturation value. Therefore  $H_{\text{eff}}^i$  and consequently the energy levels  $E_n^i$  of the ions  $i$  will be almost independent of temperature up to 20°K. The magnetic specific heat for each ion is then obtained in a standard way from the partition function, and the magnetic specific heat of the entire crystal is the sum over all the ions.

The simplest example is that for ions in an  $S$  state. Here the crystalline field splittings are negligible and the  $H_{\text{eff}}$  splits the  $(2S+1)$  manifold into equidistant

levels separated by  $E = g\beta H_{\text{eff}}$ . The partition function is

$$Z = \sum_{m=-S}^{m=+S} \exp\left(\frac{-mE}{k_B T}\right) \quad (9)$$

and the specific heat for these ions is then found to be

$$C/R = x^2 B_s'(x), \quad (10)$$

where  $B_s'(x)$  is the derivative of the Brillouin function and  $x = SE/k_B T$ .

The one-ion approximation is only valid, however, at temperatures when excited levels are appreciably populated. Hence for garnets which have their first excited level at energies below say 60 cm<sup>-1</sup>, this approximation should apply to temperatures well below 20°K. For YIG and LuIG, where  $M^{3+}$  is diamagnetic, the splittings are of the order of a few hundred cm<sup>-1</sup> and the WMF approximation should not hold in the temperature range we are concerned with. We will presently carry out a treatment in the spin-wave approximation which covers the temperature region when the alignment of the spins is nearly perfect.

### C. Spin-Wave Approximation

It is useful to consider two cases according to whether or not the orbital momentum of the rare-earth ion is zero.

#### 1. S-State Ions

Here the exchange Hamiltonian is the dominant term. For the present we neglect the effect of anisotropy and dipolar interaction, leaving only the exchange Hamiltonian to be diagonalized, hence:

$$\mathcal{H}_{\text{magn}} = -2 \sum_{\text{pairs}} J_{ij} \mathbf{S}_i \cdot \mathbf{S}_j, \quad (11)$$

We have made several simplifications in the calculation of the normal modes of this spin system. We took the case of zero external field  $H_{\text{ext}} = 0$ , although for  $S$ -state ions the effect of  $H_{\text{ext}}$  can be easily included. We also assumed that only nearest-neighbor interactions are important. Since there are in general three principal types of magnetic sublattices in the garnets, we have taken as a first approximation only six coefficients  $J_{ij}$ , corresponding to the interactions between ions in the sublattices  $i$  and  $j$ . For YIG and LuIG, where the  $c$  sublattice is nonmagnetic, only three of these parameters are needed. The use of the term  $-2J_{ij} \mathbf{S}_i \cdot \mathbf{S}_j$  also implies that the exchange field is isotropic, an assumption which is probably reasonable only for  $S$ -state ions. Finally, our calculations will be only valid at temperatures where the magnetization has not decreased substantially from its value at  $T=0$ .

Following the method of Kouvel and Brooks,<sup>14</sup> one can show that under these conditions the frequencies

<sup>13</sup> G. P. de Gennes, C. Kittel, and A. M. Portis, Phys. Rev. **116**, 323 (1959).

<sup>14</sup> J. S. Kouvel and H. Brooks, Technical Report No. 198, Cruft Laboratory, Harvard University, 1954 (unpublished).

of the normal modes of this spin system are the eigenvalues of the matrix  $\mathbf{A}$ , where

$$A_{ij} = (-2 \sum_{j'} J_{ij'} S_{j'}^z \gamma_{ij'}(0)) \delta_{ij} + 2 J_{ij} S_i^z \gamma_{ij}(\mathbf{k}), \quad (12)$$

where the indices  $i$  and  $j$  label sublattices corresponding to different ions in the unit cell,  $\delta_{ij}$  is the Kronecker delta and

$$\gamma_{ij}(\mathbf{k}) = \sum_a \exp i(\mathbf{k} \cdot \mathbf{d}_{ij}),$$

where  $\mathbf{d}_{ij}$  is a vector from an ion in the  $i$  sublattice to a nearest neighbor in the  $j$  sublattice and the sum is over all such vectors. For the rare-earth iron garnets there are 32 primitive body-centered magnetic sublattices, while for YIG there are only 20 such sublattices. In Eq. (12),  $S_i^z$  is the  $z$  component of the spin of an ion in the  $i$  sublattice and is positive or negative according to the equilibrium orientation of the spin. The eigenvalues for all the normal modes can be obtained analytically only at the center or the extreme corner of the Brillouin zone. Let us now consider the  $\mathbf{k}$  dependence of the lowest or acoustic mode. For  $\mathbf{k}=0$ , one can see that one of the eigenvalues  $E_0$  of  $\mathbf{A}$  is zero by verifying that the vector  $\psi_0$ , whose components are  $(\psi_0)_j = S_j^z$ , is a right eigenvector [i.e.,  $\sum_j A_{ij}(\psi_0)_j = 0$ ] and that  $\psi_0^a$ , whose components are  $(\psi_0^a)_j = 1$  is a left eigenvector, i.e., it solves the adjoint equation  $\sum_j (\psi_0^a)_j A_{ji} = 0$ . One can expand the eigenvalue equation in powers of the components of  $\mathbf{k}$ :

$$\mathbf{A}(\mathbf{k})\psi_n(\mathbf{k}) = E_n(\mathbf{k})\psi_n(\mathbf{k}), \quad (13)$$

where

$$\mathbf{A}(\mathbf{k}) = \mathbf{A}(0) + \mathbf{k} \cdot \nabla_k \mathbf{A}|_0 + \frac{1}{2}(\mathbf{k} \cdot \nabla_k)^2 \mathbf{A}|_0 + \dots, \quad (14)$$

$\nabla_k$  is the gradient in  $k$  space and there are similar expressions for  $\psi_n$  and  $E_n$ . The appropriate generalization of the usual perturbation formulas, which are valid for Hermitian matrices with  $\psi_n^a = \tilde{\psi}_n^*$ , is

$$E_n(k) = E_n(0) + \frac{\psi_n^a \mathbf{k} \cdot \nabla_k \mathbf{A}|_0 \psi_n}{\psi_n^a \psi_n} + (1/2) \frac{\psi_n^a (\mathbf{k} \cdot \nabla_k)^2 \mathbf{A}|_0 \psi_n}{\psi_n^a \psi_n} + \sum_m \frac{(\psi_n^a \mathbf{k} \cdot \nabla_k \mathbf{A}|_0 \psi_m)(\psi_m^a \mathbf{k} \cdot \nabla_k \mathbf{A}|_0 \psi_n)}{(\psi_n^a \psi_n)(E_n - E_m)(\psi_m^a \psi_m)} + \dots \quad (15)$$

For the iron garnets, each ion is at the center of gravity with respect to every group of neighbors governed by the same exchange integral so that  $\mathbf{k} \cdot \nabla_k \mathbf{A}|_0 \psi_0 = 0$ . Consequently the second and the last term in Eq. (15) vanish, so that it is unnecessary to solve for the other normal modes in order to find the frequency of the acoustic mode. Using the eigenvectors of the acoustic mode and Eq. (15) one finds

$$E_0(\mathbf{k}) = \hbar \omega_0 = \sum_{\text{pairs}} \frac{\frac{2}{3} J_{ij} S_i^z S_j^z d_{ij}^2}{S_{\text{tot}}} \times k^2, \quad (16)$$

where  $S_{\text{tot}} = \sum_i S_i^z$ , and the sums are taken over the sublattices  $i$ .

TABLE II. Values of the exchange integrals (in  $\text{cm}^{-1}$ ) for the iron garnets.

	YIG				LuIG		
$J_{aa}^a$				6.1			6.7
$J_{ad}^a$				25.1			25.3
$J_{dd}^a$				10.3			11.6
	GdIG	TbIG	DyIG	HoIG	ErIG	TmIG	YbIG
$J_{ed}-2J_{ea}^b$	3.5	2.8	3.0	2.2	2.2	1.5	...
$J_{ee}^b$	0.4	0.1	0.6	1.4	2.6	...	...
$J_{ea}^a$	2.6	5.4	4.8	4.7	2.3	0	27.4
$J_{ca}^a$	0.3	1.7	1.7	2.6	0.5	0	1.0

<sup>a</sup> Values calculated from Aléonard's coefficients  $n$ .

<sup>b</sup> These values are determined from Pauthenet's  $n$  coefficients. Since Pauthenet does not usually give  $n_{ea}$  and  $n_{ed}$  separately, only the combination  $J_{ed} - 2J_{ea}$  of the exchange integrals could be deduced. As can be seen, there is some inconsistency between the values of Aléonard and Pauthenet.

Taking account of the geometry of the garnet unit cell, we find<sup>15</sup>

$$\hbar \omega_0 = D a^2 k^2, \quad (17)$$

where

$$D = (1/S_{\text{tot}})[50J_{aa} - (125/4)J_{ad} + (75/4)J_{dd} + \dots], \quad (18)$$

and where  $a$  is the lattice constant. We have omitted additional terms in  $J_{ea}$ ,  $J_{ed}$ , and  $J_{ee}$  since these exchange integrals are much smaller than the iron-iron exchange integrals  $J_{aa}$ ,  $J_{ad}$ , and  $J_{dd}$ . In Table II we have tabulated values of the exchange integrals as deduced from magnetic measurements.<sup>2,3</sup> Using Aléonard's values, we find:

$$D(\text{YIG}) = 14.3 \text{ cm}^{-1}, \quad (19a)$$

$$D(\text{LuIG}) = 11.9 \text{ cm}^{-1}, \quad (19b)$$

and, assuming the iron-iron exchange integrals to be roughly the same for GdIG as for YIG,

$$D(\text{GdIG}) \approx 5 \text{ cm}^{-1}. \quad (19c)$$

It can be shown<sup>14</sup> that the specific heat per unit cell and the decrease of the spontaneous magnetization, resulting from the acoustical mode are given, respectively, as

$$C_{\text{acoustical}} = 0.113 k_B (k_B T / D)^{\frac{1}{2}}, \quad (20a)$$

$$\Delta M_{\text{acoustical}} = M(0) - M(T) = M(0)(0.0587 / S_{\text{tot}})(k_B T / D)^{\frac{1}{2}}. \quad (20b)$$

For YIG and LuIG the other branches of the spin wave spectrum should not affect the magnetic and thermal behavior below 20°K because they represent motions in which the spins within the unit cell are appreciably out of phase with one another and hence have an energy comparable to  $kT_e$  where  $T_e$  is 550°K. Douglass<sup>16</sup> has made an exact calculation of the fre-

<sup>15</sup> The details of this calculation, which takes account of the sublattice structure in the garnets are given in the Ph.D. thesis of A. B. Harris, Harvard University, 1961, (unpublished) and will be presented in a forthcoming technical report.

<sup>16</sup> R. L. Douglass, Phys. Rev. 120, 1612 (1960).

quency of all the modes for  $\mathbf{k}=0$  and at the extreme corner of the Brillouin zone. His calculations indeed show that the energy of the optical modes is of the order of 100–500  $\text{cm}^{-1}$ . He also gives an expression for  $D$  in agreement with ours.<sup>17</sup>

For GdIG, on the other hand, we cannot neglect the influence of all the optical modes. This is because  $J_{ca}$  and  $J_{cd}$  correspond to exchange fields which give splittings of the order of 20–50  $\text{cm}^{-1}$ , and which should influence greatly the specific heat at low temperatures as mentioned in the introduction.

In order to carry out a calculation of the positions of these low optical modes, we write

$$\mathbf{A} = \mathbf{A}_{\text{YIG}} + \mathbf{V}, \quad (21)$$

where  $\mathbf{A}_{\text{YIG}}$  includes only the effect of the iron-iron exchange integrals and  $\mathbf{V}$  is therefore a small perturbation on  $\mathbf{A}_{\text{YIG}}$ .<sup>18</sup> Since for small values of  $\mathbf{k}$ , the difference between the energy of these low optical modes and the acoustical mode is much less than the energy of optical modes for YIG, it is necessary to use degenerate perturbation theory. The result of a first-order perturbation calculation is that there are 11 closely spaced low optical modes whose frequency is not very dependent on  $\mathbf{k}$  and whose average frequency is

$$\bar{\omega}_1 = (1/\hbar)[20J_{ac} - 10J_{dc} + 8J_{cc}S_c], \quad (22)$$

where  $S_c$  is the spin of an  $M^{3+}$  ion. Using the relation between the exchange integral and the molecular field coefficients, it can be shown that

$$\hbar\bar{\omega}_1 = g\beta H_{\text{eff}} = E_1, \quad (23)$$

where  $H_{\text{eff}}$  is the WMF acting on the rare-earth ion. The frequency of a twelfth low optical mode is highly dependent on  $\mathbf{k}$ . At  $\mathbf{k}=0$  we find

$$\hbar\omega_2 = g\beta H_{\text{eff}}(6S_c - 5)/5. \quad (24)$$

This mode is the exchange mode as already found by Kaplan and Kittel<sup>19</sup> for a two sublattice system. At the extreme corners of the Brillouin zone its frequency coincides with that of the other eleven modes.

*Note added in proof.* Since this paper was submitted, detailed calculations of the spin wave spectrum for YIG and GdIG in  $k$  space have been carried out by one of us (A.B.H.). For  $(6S_c - 5) < 0$ , the low optical mode does indeed become degenerate with the other optical modes at the extreme corners of the Brillouin zone. For  $(6S_c - 5) > 0$ , the frequency of this mode increases rapidly with  $k$ . In this case, however, the frequency of the acoustical mode approaches  $\hbar\bar{\omega}_1$ , as  $k$  approaches the corners of the Brillouin zone. In either case, the specific heat can be described satisfactorily as arising effectively from 12 modes  $\hbar\bar{\omega}_1$  and an acoustical mode. Equations (27) and (28) are still useful and differ little from the more accurate result.

The specific heat per unit cell arising from these excitations is

$$C_{\text{optical}} = k_B \sum_{\text{modes}} \int_{\text{Brillouin zone}} \frac{x^2 e^{-x}}{(e^{-x} - 1)^2} \frac{V}{8\pi^3} dk_x dk_y dk_z, \quad (25)$$

where  $V$  is the volume of the unit cell and  $x = \hbar\omega(\mathbf{k})/k_B T$ . The integration can be performed immediately for the 11 low optical modes whose frequency dependence of  $\mathbf{k}$  we neglect, and gives a contribution

$$22k_B \left( \frac{\hbar\bar{\omega}_1}{k_B T} \right)^2 \frac{e^{-\hbar\bar{\omega}_1/k_B T}}{(1 - e^{-\hbar\bar{\omega}_1/k_B T})^2} \equiv 22k_B \epsilon \left( \frac{\hbar\bar{\omega}_1}{k_B T} \right), \quad (26)$$

where  $\epsilon(\hbar\bar{\omega}_1/k_B T)$  is the Einstein function. The calculation of the specific heat due to the twelfth mode is more difficult, since the exact variation of  $\omega_2$  with  $\mathbf{k}$  is not readily determined. For  $\text{Gd}^{3+}$ ,  $\omega_2(k=0) = (16/5)\bar{\omega}_1$  and the average of  $\omega_2$  must lie somewhere between  $\bar{\omega}_1$  and  $(16/5)\bar{\omega}_1$ . Tinkham<sup>18</sup> has made a simplified calculation which indicates that the effective value of  $\omega_2$  should be close to  $\bar{\omega}_1$ . We hence make the approximation that the energy of the 12th mode is the same as that of the eleven other modes. Since there are 4 molecules per unit cell, we have per mole

$$C_{\text{optical}} = 6R\epsilon(\hbar\bar{\omega}_1/k_B T). \quad (27)$$

For  $\text{Gd}^{3+}$  the exact frequencies of all the modes for  $\mathbf{k}=0$  have been determined by Dreyfus<sup>20</sup> in terms of the exchange integrals. The numerical values of these frequencies, obtained by a fit with our calorimetric data, correspond to temperatures between 26 and 46°K. Some of the accuracy of his spin-wave calculation is lost when his results are applied to specific heat, as the frequency variation of the modes with  $\mathbf{k}$  is probably comparable to their separation.

Let us now consider the specific heat due to the acoustical mode. While for YIG the expressions (20a) and (20b) are adequate below about 4°K, this is not so for GdIG where higher order terms in  $T^{5/2}$  and even  $T^{7/2}$  have to be taken into account. Harris (to be published) finds the specific heat of the acoustical mode to be

$$C_{ac}(\text{GdIG}) \approx 0.113k_B \left( \frac{k_B T}{D(\text{GdIG})} \right)^{\frac{3}{2}} \times \left[ 1 + 7.35 \frac{k_B T}{\hbar\bar{\omega}_1} \left| \frac{6S_c}{5 - 6S_c} \right| + O(T^2) \dots \right] \dots \quad (28)$$

Hence the total magnetic specific heat per mole of GdIG is

$$C = \frac{1}{4}NC_{ac}(\text{GdIG}) + 6R\epsilon(\hbar\bar{\omega}_1/k_B T). \quad (29)$$

<sup>17</sup> H. Meyer and A. B. Harris, J. Appl. Phys. **31**, 49S (1960).

<sup>18</sup> M. Tinkham, Phys. Rev. **124**, 311 (1961).

<sup>19</sup> J. Kaplan and C. Kittel, J. Chem. Phys. **21**, 760 (1953).

<sup>20</sup> B. Dreyfus, *Proceedings of the Seventh International Conference on Low-Temperature Physics, Toronto, 1960* (University of Toronto Press, Toronto, 1961), p. 127.

Let us now estimate the effects of anisotropy and dipolar interactions on the spin-wave spectrum. Let us take  $K$  to be the first-order anisotropy constant and  $V$  the molar volume. We note that both  $K(M/V)$  and  $\frac{4}{3}\pi(M/V)$  are much less than the exchange field acting on the gadolinium ions, and hence the low optical modes with the exception of  $\omega_2$  will not be significantly influenced by these perturbations. The acoustic branch of the spin-wave spectrum, on the other hand, will be more affected especially for small values of  $\mathbf{k}$ . Let us consider a spherical volume element which is small enough so that the magnetization is essentially constant therein. The dipolar fields from the rest of the sample result from the magnetic poles on the surface of the spherical volume element, but not, however, from the surface of the sample, which is assumed to be unmagnetized. We assume, therefore, that the effect of the rest of the sample on the small volume element is equivalent to an effective field  $H = \frac{4}{3}\pi(M/V)$ . We can now use the dispersion relation for a magnetized sample,<sup>21</sup>

$$(\hbar\omega)^2 = [Da^2k^2 + g\beta(H - \frac{4}{3}\pi M/V)] \times [Da^2k^2 + g\beta(H - \frac{4}{3}\pi M/V) + 4\pi g\beta(M/V) \sin^2\theta_k], \quad (30)$$

where of course we should take  $H = \frac{4}{3}\pi(M/V)$ .  $\theta_k$  is the angle between the magnetic field and  $\mathbf{k}$ . Thus far we have neglected the anisotropy. However, since  $H_{\text{anisotropy}}$  is much less than  $\frac{4}{3}\pi(M/V)$ ,<sup>22</sup> the principal distortions in the spin-wave spectrum will be caused by dipolar interaction as shown by Herring and Kittel.<sup>23</sup> Therefore,

$$(\hbar\omega)^2 = Da^2k^2 [Da^2k^2 + 4\pi g\beta(M/V) \sin^2\theta_k]. \quad (31)$$

If this expression is substituted into the appropriate formula for the specific heat, one finds that for  $g\beta M/k_BTV \ll 1$ ,

$$C_{\text{acoustical}}^* = C_{\text{ac}} \left[ 1 - 1.6 \frac{g\beta M}{k_BTV} + \dots \right], \quad (32)$$

where  $C_{\text{ac}}$  is the specific heat given by Eq. (20a) or Eq. (28). At 1.3°K, which was the lowest temperature reached in our specific heat measurements,  $(g\beta M/k_BTV)$  was 0.08 for GdIG and 0.025 for YIG. Hence, the effect of the dipolar interaction was expected to be small. Calculations of the effect of dipolar interaction in a large magnetic field have been carried out by Edmonds.<sup>24</sup>

## 2. Non-S-State Ions. Inverted Multiplets

When the orbital angular momentum  $L$  is not zero, it is necessary to consider the spin-orbit interaction and

the crystalline field potential in addition to the exchange interaction. Thus, the Hamiltonian can be written approximately as

$$\mathcal{H}_{\text{magn}} = V_{\text{crystal}} - 2 \sum_{\text{pairs}} J_{ij} \mathbf{S}_i \cdot \mathbf{S}_j + A \mathbf{L} \cdot \mathbf{S}, \quad (33)$$

where we have not yet indicated the form of the crystalline field potential. For inverted multiplets, i.e., for the second half of the rare earth series,  $A$  is negative.<sup>25</sup> As a result the first excited multiplet lies sufficiently far above the ground multiplet so that  $J$  is a good quantum number in this multiplet.<sup>26</sup> Thus, we are left with the following Hamiltonian

$$\mathcal{H}_{\text{magn}} = V_{\text{crystal}} - 2 \sum_{\text{pairs}} J_{ij} \mathbf{S}_i \cdot \mathbf{S}_j, \quad (34)$$

where only that part of the Hamiltonian which is diagonal in  $J$  need be considered. In analogy with the results for  $S$ -state ions, one might expect contributions to the specific heat from both acoustic and the optical branches of the spin-wave spectrum. In the Appendix we give a crude argument which shows that in this case there will be a negligibly small contribution from the acoustic branch. Let us now consider the position of the 12 low-lying optical modes, at first neglecting anisotropy. We expect again to have 11 nearly degenerate modes whose frequency is given by Eq. (23). As remarked in the Appendix, one should substitute for  $S_0$  the effective spin value  $\frac{1}{2}$  or at most 1. Using Eq. (24), one sees that  $\omega_2$  will lie below the other eleven modes. As a result of the anisotropy, there are two inequivalent types of  $c$  sites and preliminary calculations show that the group of eleven modes splits up into two groups of 5 modes, corresponding to the two inequivalent sites, and one mode lying in between. The position of the exchange mode has not yet been determined but for the special case of YbIG, Tinkham<sup>18</sup> has shown that it lies below the others. If its average value is low enough, then it should affect the specific heat noticeably at the lowest temperatures, although Tinkham's calculations indicate that this should not be so. At higher temperatures, the specific heat is not sensitive to the exact position of this mode, which is shown to approach the other ones<sup>18</sup> and there the WMF approximation is expected to be valid.

The problem is thus reduced to a one-ion problem. One only needs to take into account the energy levels of the rare-earth ion under the combined influence of the crystalline field and the effective magnetic field. Only a few solutions have been reported so far. White and Andelin<sup>27</sup> have assumed that the potential could be represented by a fourth-order cubic term. Using an electronic computer, they calculated the energy levels

<sup>21</sup> H. Suhl, Proc. Inst. Radio Engrs. **44**, 1270 (1956).

<sup>22</sup> G. P. Rodrigue, H. Meyer, and R. V. Jones, Suppl. J. Appl. Phys. **31**, No. 5, 376 (1960).

<sup>23</sup> C. Herring and C. Kittel, Phys. Rev. **81**, 869 (1951).

<sup>24</sup> D. T. Edmonds (private communication).

<sup>25</sup> J. H. Van Vleck, *Theory of Electric and Magnetic Susceptibilities* (Oxford University Press, New York, 1932).

<sup>26</sup> L. I. Schiff, *Quantum Mechanics* (McGraw-Hill Book Company, New York, 1955), p. 287 ff.

<sup>27</sup> R. L. White and J. Andelin, Phys. Rev. **115**, 1435 (1959).

of the rare-earth ion for various values of the relative strength of the two fields. Their results, however, are often not compatible with the interpretation of our specific heat data. It should be remarked that their calculations assumed that the effective field lay in a  $[100]$  or in a  $[110]$  direction rather than in a  $[111]$  direction, as is actually the case. Also, since the local symmetry axes do not coincide with the crystal axes, one should calculate the splittings for each of the two inequivalent sites. For one of these sites the field lies along a local  $[\sqrt{\frac{2}{3}} 0 \sqrt{\frac{1}{3}}]$  direction and for the other site a local  $[0 \sqrt{\frac{2}{3}} \sqrt{\frac{1}{3}}]$  direction. At present, the only statement one can make is that the specific heat should be interpreted under the assumption that there are two inequivalent sites whose energy level schemes may not be the same.

In the special case of YbIG some progress has been made.<sup>27a</sup> Here it has been established that the crystalline field splittings are much larger than those caused by the exchange field.<sup>5</sup> For  $\text{Yb}^{3+}$  the effect of noncubic terms in the crystalline field potential on the wave functions of the doublet vanishes in first order, so that the exact form of the crystalline field is not too important. Therefore, we expect that the  $g_{\text{eff}}$  values of the lowest doublet of  $\text{Yb}^{3+}$  should be the same in YbIG as in isostructural ytterbium gallium garnet for which  $g_x = 3.73$ ,  $g_y = 3.60$ ,  $g_z = 2.85$ .<sup>28</sup> In an effective magnetic field  $H_{\text{eff}}$  the energy levels are split by an amount

$$E_l = \beta H_{\text{eff}} (g_x^2 l^2 + g_y^2 m^2 + g_z^2 n^2)^{\frac{1}{2}}, \quad (35)$$

where  $l$ ,  $m$ , and  $n$  are the direction cosines.

Since the effective field lies in turn along local directions mentioned above, one finds, using the  $g$  values quoted above, that the splittings  $E_l$  and  $E_{l'}$  are, respectively,  $3.46\beta H_{\text{eff}}$  and  $3.37\beta H_{\text{eff}}$ , from which one calculates the specific heat in the usual way.

One can also calculate the magnetization as a function of temperature, knowing the  $g$  values. However, it is necessary to take into account the contribution of the off-diagonal elements of the magnetic moment. Ayant and Thomas<sup>29</sup> have calculated the magnetization of  $\text{Yb}^{3+}$  assuming an isotropic  $g_{\text{eff}}$  tensor. Using their calculations one has:

$$M(\text{Yb}^{3+}) = \frac{1}{2} N g_{\text{eff}} \beta \left\{ \frac{g_{\text{eff}} \beta H_{\text{eff}}}{15A} + \tanh \left( \frac{g_{\text{eff}} \beta H_{\text{eff}}}{2k_B T} \right) \right\}, \quad (36)$$

where  $20A$  is the separation between the lowest doublet and the excited quartet which is slightly split by non cubic terms in the crystalline potential. Taking  $A$  to be  $28 \text{ cm}^{-1}$ ,<sup>5</sup>  $g_{\text{eff}} = 24/7$ , and using magnetization data at

<sup>27a</sup> Note added in proof. The energy levels of terbium doped YIG have been determined by Dillon and Walker [Phys. Rev. **124**, 1401 (1961)].

<sup>28</sup> D. Boakes, G. Garton, D. Ryan, and W. P. Wolf, Proc. Phys. Soc. (London) **A74**, 663 (1959); J. W. Carson and R. L. White, J. Appl. Phys. **31**, 535 (1960).

<sup>29</sup> Y. Ayant and G. Thomas, Compt. rend. **250**, 2688 (1960).

low temperatures,<sup>2</sup> we find  $g_{\text{eff}} \beta H_{\text{eff}} = 25.5 \text{ cm}^{-1}$ , almost independent of temperature below  $70^\circ\text{K}$ .

One can also estimate the splitting of the lowest doublet in YbIG by assuming that the exchange integrals are the same in YbIG as in GdIG. If the exchange Hamiltonian is written as  $\beta \mathbf{H}_{\text{ex}} \cdot \mathbf{S}$ , this implies that  $\mathbf{H}_{\text{ex}}$  is the same for both garnets. Elementary calculations show that

$$E_1(\text{Yb}^{3+}) = E_1(\text{Gd}^{3+}) \frac{g_L - 1}{g_L} g_{\text{eff}} = (3/7) E_1(\text{Gd}^{3+}), \quad (37)$$

where  $E_1(M^{3+})$  is the splitting for the  $M$  ion in MIG and  $g_L$  is the Landé factor of ytterbium. This type of calculation is only possible when the exchange field does not cause admixing of different crystalline states.

### 3. Non-S-States. Normal Multiplets

Of the rare earths preceding gadolinium in the periodic table, only samarium and europium form stable iron garnets. The other rare earths can be introduced in small concentrations to form mixed garnets of the form  $5\text{Fe}_2\text{O}_3 \cdot 3(\text{M}_x\text{Y}_{1-x})_2\text{O}_3$ , where  $x$  is the relative concentration of the rare-earth ions. Since  $S$  and  $J$  are normally antiparallel for these ions, the magnetization of the  $c$  sublattice is coupled ferromagnetically to the resultant of the  $a$  and  $d$  sublattices. Observations of this effect have been made by Goldring, Schieber and Vager<sup>30</sup> and were first explained by Wolf.<sup>31</sup> For  $\text{Eu}^{3+}$  and  $\text{Sm}^{3+}$  the separation between the lowest and the first excited multiplet is much smaller than for the other rare earths,<sup>25</sup> and the treatment of the crystalline field becomes difficult. Wolf and Van Vleck<sup>32</sup> have interpreted magnetization data for EuIG under the assumption that the  $J=1$  multiplet is not significantly split by the crystalline field. For  $\text{Sm}^{3+}$ , the lowest multiplet  $J=\frac{5}{2}$  is split by the crystalline field into 3 doublets which in turn are split by the exchange field. Perturbation calculations must be carried to a high order, as it is no longer true that

$$\mathcal{H}_{\text{s.o.}} \gg V_{\text{crystal}} \gg \mathcal{H}_{\text{exchange}}.$$

Thus far there are no such published calculations of the energy levels. Such a theory would have to explain the presence of large splittings as deduced from specific heat data (see Sec. IV B 4.), and on the other hand the failure of  $\text{Sm}^{3+}$  to contribute to the magnetization in SmIG.<sup>2</sup>

### D. The Nuclear Specific Heat

If quadrupole interaction is neglected, and in the absence of an applied magnetic field, the nuclear

<sup>30</sup> G. Goldring, M. Schieber, and Z. Vager, J. Appl. Phys. **31**, 2057 (1960).

<sup>31</sup> W. P. Wolf, J. Appl. Phys. **32**, 742 (1961).

<sup>32</sup> W. P. Wolf and J. H. Van Vleck, Phys. Rev. **118**, 1490 (1960).



Hamiltonian can be written in first approximation as<sup>33</sup>

$$\mathcal{H}_{\text{nuc}} = P\{\mathbf{L} \cdot \mathbf{I} + \eta[(L+1)\mathbf{L} \cdot \mathbf{S} \cdot \mathbf{I} - \frac{3}{2}(\mathbf{L} \cdot \mathbf{S})(\mathbf{L} \cdot \mathbf{I}) - \frac{3}{2}(\mathbf{L} \cdot \mathbf{I})(\mathbf{L} \cdot \mathbf{S})]\} + \xi \mathbf{S} \cdot \mathbf{I}, \quad (38)$$

where  $P$ ,  $\eta$ , and  $\xi$  are constants.  $\xi$  is different from zero only when there are  $s$  electrons present.

When  $L=0$ , and there are no unpaired  $s$  electrons, (38) gives no nuclear splittings. It is then necessary to take account of the polarization of the  $s$  orbitals. Since the degree of polarization depends on the environment,<sup>34</sup> one can only make a crude estimate of the size of the nuclear splittings for ions in the garnet lattice. Measurements of the Mössbauer effect and nuclear resonance<sup>35</sup> show that the nuclear splittings of Fe<sup>57</sup> in the iron garnets are too small to affect the specific heat above 1°K. Since the effective fields acting on the rare-earth ions are weaker than those acting on the iron ions, one would expect the polarization of the  $s$  orbitals to be smaller for Y, Gd, and Lu than for Fe. We have estimated that the nuclear specific heat of these ions would be negligible above 1°K.

For non- $S$ -state ions, on the other hand, the nuclear Hamiltonian is effective in first order and hence will produce an observable nuclear specific heat above 1°K. Insofar as  $J$  remains a good quantum number in the presence of a crystalline field, one can write

$$\mathcal{H}_{\text{nuc}} = \lambda \beta (\mathbf{L} + 2\mathbf{S}) \cdot \mathbf{I} = \lambda \mathbf{u} \cdot \mathbf{I}, \quad (39)$$

where  $\lambda$  depends only on the nuclear constants and the Landé factor and is independent of the environment.<sup>36</sup> Since in general  $\mathcal{H}_{\text{ex}} \gg \mathcal{H}_{\text{nuc}}$ , the energy levels of the rare-earth ions are

$$E_{nm} = E_n + \lambda \mu_n m, \quad (40)$$

with  $\mu_n = |\langle n | \mathbf{u} | n \rangle|$ , where  $m$  varies from  $-I$  to  $I$  and the electronic state is labeled with the index  $n$ . At temperatures where one expects an appreciable specific heat from nuclear interaction, the magnetic moment  $\mu$  of the ion is that of the lowest electronic state. The resulting specific heat is

$$\frac{C_{\text{nuc}}}{R} = \left( \frac{\Delta I}{k_B T} \right)^2 B_I' \left( \frac{\Delta I}{k_B T} \right), \quad (41a)$$

and when  $\Delta I \ll k_B T$  one finds<sup>34</sup>

$$\frac{CT^2}{R} = \frac{I(I+1)}{3} \left( \frac{\Delta}{k_B} \right)^2, \quad (41b)$$

where  $\Delta = \lambda \mu$  is the separation between successive

TABLE III. Calculated nuclear specific heat of rare-earth iron garnets.

Isotope	Abundance	$I$	$\lambda \beta$ (in cm <sup>-1</sup> )	$\Delta$ (in cm <sup>-1</sup> )	$CT^2 \times 10^3$ (in J deg/mole)
Tb <sup>169</sup>	100%	$\frac{3}{2}$	0.012	0.084	908
Dy <sup>161</sup>	18.88	$\frac{5}{2}$	0.00280	0.020	81.1
Dy <sup>163</sup>	24.97	$\frac{5}{2}$	0.00397	0.028	
Ho <sup>165</sup>	100	$\frac{7}{2}$	0.022	0.139	10400
Er <sup>167</sup>	22.94	$\frac{7}{2}$	0.00355	0.019	37.5
Yb <sup>171</sup>	14.34	$\frac{5}{2}$	0.0267	0.045	15.8
Yb <sup>173</sup>	16.18	$\frac{5}{2}$	0.0075	0.012	

The values of  $\lambda \beta$  which are equal to the ratio  $A_z/g_z = A_z/g_z$  obtained from paramagnetic resonance data were compiled from the article by Bowers and Owen, Reports on Progress in Physics (The Physical Society London, 1955) 18, p. 304, and from references 37 and 38. The values of  $\Delta$  are somewhat uncertain due to the possible error in the electronic magnetic moment  $\mu$ . See reference 2.

nuclear levels. One must then average the specific heat over all the isotopes. In order to estimate the size of the nuclear specific heat, we can use the values of  $\lambda$  as determined from paramagnetic resonance in the rare earth ethylsulphates<sup>26</sup> and acetates<sup>37,38</sup> and of  $\mu$  as estimated from Pauthenet's magnetization data at low temperatures. If the electronic magnetic moments were aligned parallel to the effective field, we would have at  $T=0$

$$\mu = M(M^{3+})/6N = [M(\text{MIG}) + M(\text{YIG})]/6N. \quad (42)$$

However the crystalline field has the effect of canting the spins so that  $\mu$  will be actually somewhat larger than we would expect from magnetization data. This enhancement will be larger the more anisotropic the  $g_{\text{eff}}$  values are. For example, using the  $g_{\text{eff}}$  values of Dy<sup>3+</sup> in the gallium garnet as determined by Wolf and co-workers,<sup>39</sup> we find that due to the canting, our estimates for  $\mu$  may be about 20% too low. In Table III, we give our estimates of the nuclear specific heat, neglecting the canting of the spins.

## E. Summary

In view of the above calculations let us summarize the expected behavior of the specific heats of the iron garnets.

For both YIG and LuIG we expect that at low enough temperatures

$$C = 7.78 \times 10^4 (T/\Theta)^3 + 0.235 (k_B T/D)^{\frac{1}{2}} \text{ J/M deg}, \quad (43)$$

where  $D$  should be about the same for both garnets and  $\Theta$  should be 15% larger for YIG than for LuIG. At higher temperatures, when (43) is no longer valid, the

<sup>33</sup> B. Bleaney and K. W. H. Stevens, *Reports on Progress in Physics* (The Physical Society, London, 1953), Vol. 16, p. 108.

<sup>34</sup> W. Marshall, *Phys. Rev.* **110**, 1280 (1958).

<sup>35</sup> G. Alf and G. K. Wertheim, *Phys. Rev.* **122**, 1414 (1961); E. L. Boyd, L. J. Brunner, J. I. Budnick, and R. J. Blume, *Bull. Am. Phys. Soc.* **6**, 159 (1961).

<sup>36</sup> R. J. Elliott and K. W. H. Stevens, *Proc. Roy. Soc. (London)* **219A**, 387 (1953).

<sup>37</sup> A. H. Cooke and J. G. Park, *Proc. Phys. Soc. (London)* **A69**, 282 (1956).

<sup>38</sup> J. M. Baker and B. Bleaney, *Proc. Phys. Soc. (London)* **A68**, 1090 (1955).

<sup>39</sup> M. Ball, G. Garton, M. J. Leask, D. Ryan, and W. P. Wolf, *J. Appl. Phys.* **32**, 376S (1961).

TABLE IV. Specific heat results for several iron garnets in J/mole deg. One mole has the formula  $3M_2O_3 \cdot 5Fe_2O_3$ .

$T$ (°K)	YIG	SmIG	GdIG	TbIG	DyIG	HoIG	ErIG	YbIG	LuIG
1.30	0.00298		0.0393					0.0151	0.00319
1.50	0.00396	0.481	0.0444	0.583				0.0148	0.00448
1.75	0.00548	0.532	0.0523	0.478		5.30		0.0150	0.00658
2.00	0.00724	0.542	0.0614	0.422	0.0485	4.22		0.0190	0.00917
2.25	0.00939	0.537	0.0711	0.387	0.0518	3.42	0.084	0.0264	0.0124
2.50	0.01182	0.513	0.0825	0.369	0.0585	2.82	0.198	0.0392	0.0163
2.75	0.01475	0.492	0.0992	0.367	0.073	2.43	0.352	0.0645	0.0211
3.00	0.0182	0.477	0.123	0.366	0.103	2.07	0.602	0.110	0.0268
3.25	0.0221	0.456	0.161	0.396	0.144	1.80	0.948	0.187	0.0334
3.50	0.0266	0.443	0.224	0.425	0.207	1.60	1.40	0.308	0.0412
3.75	0.0315	0.446	0.311	0.467	0.290	1.45	1.95	0.475	0.0498
4.00	0.0373	0.458	0.430	0.520	0.398	1.35	2.61	0.705	0.0601
4.5	0.0532	0.516	0.84	0.656	0.732	1.26	4.13	1.40	0.0846
5.0	0.0701	0.613	1.39	0.823	1.204	1.38	5.90	2.32	0.1110
5.5	0.0890	0.760	2.18	1.038	1.79	1.71	7.58	3.38	0.1405
6.0	0.115	0.985	3.16	1.27	2.46	2.16	9.41	4.63	0.178
6.5	0.140	1.25	4.26	1.63	3.31	2.67	11.26	6.11	0.223
7.0	0.170	1.55	5.46	2.01	4.20	3.44	13.26	7.66	0.274
7.5	0.207	1.92	6.92	2.42	5.24	4.37	15.22	9.37	0.340
8.0	0.252	2.39	8.29	2.94	6.49	5.40	17.20	11.09	0.415
8.5	0.302	2.92	9.88	3.53	7.73	6.73	19.38	12.58	0.507
9.0	0.358	3.51	11.69	4.14	8.99	8.29	21.6	14.04	0.617
9.5	0.425	4.15	13.61	4.84	10.36	9.91	23.7	15.46	0.737
10.0	0.495	4.86	15.49	5.49	11.72	11.54	25.6	16.64	0.870
11.0	0.660	6.22	19.1	6.98	14.63	15.00	29.7	18.63	1.200
12.0	0.862	7.90	22.3	8.65	17.7	19.1	33.6	20.20	1.64
13.0	1.120	9.66	25.2	10.56	20.7	23.3	38.0	21.71	2.20
14.0	1.415	11.23	28.4	12.43	24.0	27.3	42.0	22.6	2.93
15.0	1.770	13.53	31.3	14.68	27.1	31.4	45.5	23.6	3.79
16.0	2.185	15.85	34.3	17.39	29.7	35.4	49.0	24.5	4.80
17.0	2.69	18.15	37.2	20.15		39.6	52.6	25.2	6.02
18.0	3.27	20.65	40.2	23.4		44.2	55.9	26.0	7.42
19.0	4.01	23.3	43.1	26.8		48.3	58.6	26.9	8.96
20.0	4.87	26.1	45.8	30.5		52.4	61.6	27.8	10.60
21.0	5.90		48.5	34.5		56.5	64.7		12.43

lattice specific heat will then be taken as

$$C_{\text{latt}} = C - AT^{\frac{3}{2}}, \quad (44)$$

i.e., any deviations from (43) are assumed to be due to a break down of the  $T^{\frac{3}{2}}$  law. Since the  $T^{\frac{3}{2}}$  term is about 50 times larger than the spin-wave term at 20°K, it would be necessary to postulate an anomalously large departure from the  $T^{\frac{3}{2}}$  law to account for the excess specific heat at this temperature. We shall also assume that the lattice specific heat of the other rare earth garnets is the same as that of LuIG.

For GdIG we again expect no nuclear specific heat. However, we expect contributions from the low optical modes, which correspond to reversing the spin of a gadolinium ion in the exchange field. Thus in the spin-wave approximation the specific heat per mole garnet should be

$$C = C_{\text{latt}} + C_{\text{ao}}(\text{GdIG}) + 6R\epsilon(\hbar\omega_1/k_B T), \quad \text{for } k_B T \ll \hbar\omega_1, \quad (45a)$$

and in the Weiss molecular field approximation we have 8 equally spaced levels giving a specific heat:

$$C = C_{\text{latt}} + 6R(7E_1/2k_B T)^2 B_{7/2}'(7E_1/2k_B T), \quad \text{for } k_B T \sim E_1. \quad (45b)$$

For  $k_B T \lesssim \hbar\omega_1/2$ , the Einstein function  $\epsilon(\hbar\omega_1/k_B T)$  and the second term in Eq. (45b) give the same result.

For the rare-earth ions not in  $S$  states, the large crystalline field is expected to have two effects: first, the acoustic branch of the spin-wave spectrum will not give an appreciable specific heat and secondly, the two inequivalent sites may have different splittings. Except at the lowest temperatures, the exact position of the exchange mode  $\omega_2$  does not affect the specific heat noticeably. Therefore we use the WMF approximation where we expect

$$C - C_{\text{latt}} = C_{\text{nuc1}} + 3C_1 + 3C_2, \quad (46)$$

where

$$C_i = RT(d^2/dT^2)T \ln Z_i$$

and

$$Z_i = \sum_m \exp(-E_m^i/k_B T).$$

$E_m^i$  is the  $m$ th energy level of the  $i$ th inequivalent site.  $C_{\text{nuc1}}$  is given by Eq. (40). In order to make rough determinations of the positions of the higher energy levels from the experimental data, functions of the type given in Eq. (46) were tabulated.

#### IV. RESULTS

The results of our specific heat measurements on the iron garnets are presented and discussed below. Pre-

liminary reports of these experiments have already been published.<sup>17,40</sup> Smoothed values of the specific heat are presented in Table IV while the original data will be tabulated in a forthcoming technical report.

### A. S-State Ions

#### 1. YIG and LuIG

We have made measurements on two samples of YIG, the first prepared at the Gordon McKay Laboratory, the second prepared by Dr. J. Kunzler at Bell Telephone Laboratories. The results on our first sample, already reported,<sup>17</sup> were subsequently discarded, because of possible contamination either by oxide impurities or by a remanent of exchange gas. We present here the results of measurements conducted on the second sample.

Since yttrium and lutetium are both in *S* states, the specific heat will consist of contributions from the lattice and the acoustic branch of the spin-wave spectrum, as given in Eq. (43). Consequently, we have plotted  $CT^{-3/2}$  vs  $T^{3/2}$  for these garnets in Figs. 1 and 2. The values of  $\Theta$  and  $D$  were deduced from the data below 6°K, in which region Eq. (43) was found to be valid, and are given in Table V along with values deduced from experiments of other workers. The value of  $D$  obtained from Pauthenet's magnetization measurements<sup>2</sup> is not particularly reliable, since his results are not well represented by a  $T^{3/2}$  law. Aléonard<sup>3</sup> quotes values of the exchange coefficients extrapolated to  $T=0$  from temperatures above the Curie point. It is possible that the uncertainty in this extrapolation is responsible for the discrepancy between the value of  $D$  as calculated from these interaction coefficients and that found by heat capacity experiments. Since the calorimetric determination of  $D$  is the more direct, we assume it to be the more reliable. There is, however, some dis-

TABLE V. Values of  $D$  and  $\Theta$  for YIG and LuIG.

	$D$ (cm <sup>-1</sup> )	$\Theta$ (°K)
YIG		
Specific heat (present work)	$20.8 \pm 1.7$	$572 \pm 14$
Specific heat (Kunzler <sup>a</sup> )	27.1	510
Specific heat (Edmonds <sup>b</sup> )	16.7	454
Specific heat (Shinozaki <sup>c</sup> )	26.4	538
	27.8	567
Sound Velocity (McSkimin <sup>d</sup> )	...	566
Magnetization (Pauthenet <sup>e</sup> )	18	...
Susceptibility (Aléonard <sup>f</sup> )	14	...
Microwave Instability <sup>g</sup>	~30	...
Microwave Instability <sup>h</sup>	~30	...
LuIG		
Specific heat (present work)	$27.1 \pm 2.2$	$458 \pm 11$
Susceptibility (Aléonard <sup>f</sup> )	11.9	...

<sup>a</sup> See reference 42.

<sup>b</sup> See reference 41.

<sup>c</sup> See reference 43.

<sup>d</sup> See reference 44.

<sup>e</sup> See reference 2.

<sup>f</sup> See reference 3.

<sup>g</sup> See reference 45.

<sup>h</sup> See reference 46.

<sup>40</sup> A. B. Harris and H. Meyer, *Proceedings of the Seventh International Conference on Low-Temperature Physics*, Toronto, 1960 (University of Toronto Press, Toronto, 1961), p. 125.

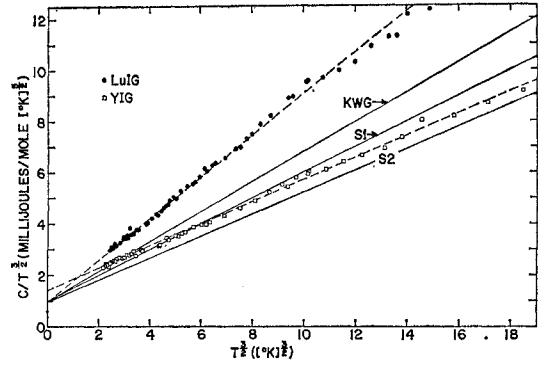


FIG. 1. The specific heat of YIG and LuIG between 1.5 and 6°K plotted as  $C/T^{3/2}$  vs  $T^{3/2}$ . The line KWG represents the results for YIG of Kunzler, Walker, and Galt. The lines  $S_1$  and  $S_2$  represent the data of Shinozaki for YIG.

crepancy even among the calorimetric results of the various workers, both in  $D$  and in  $\Theta$ . The total specific heat measured by Edmonds and Petersen<sup>41</sup> was about twice that of the other workers, probably as a result of impurities. It is expected that  $D$  should be the same for both YIG and LuIG, whereas  $\Theta$  should be about 15% less for LuIG than for YIG. It is somewhat surprising that our value of  $D$  for YIG does not agree more closely with the most reliable<sup>42,43</sup> of the other values. More conclusive measurements at lower temperatures and on other samples will be undertaken shortly to resolve this discrepancy.

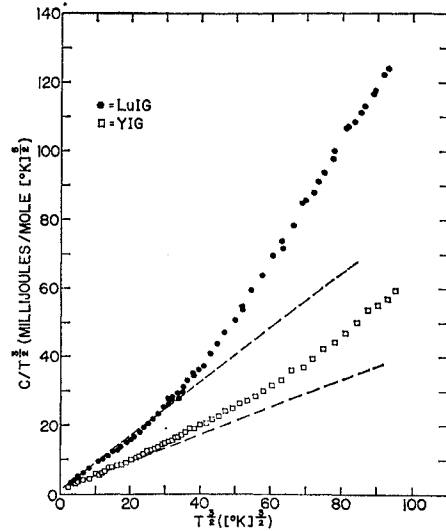


FIG. 2. The specific heat of YIG and LuIG between 1.5° and 21°K plotted as  $C/T^{3/2}$  vs  $T^{3/2}$ . The dashed curves give the extrapolation of the results for temperatures below 6°K. The departure of the data from this extrapolation is probably due to the excitation of low optical lattice modes.

<sup>41</sup> D. Edmonds and R. Petersen, *Phys. Rev. Letters* **2**, 499 (1959).

<sup>42</sup> J. E. Kunzler, L. R. Walker, and J. R. Galt, *Phys. Rev.* **119**, 1609 (1960).

<sup>43</sup> S. S. Shinozaki, *Phys. Rev.* **122**, 388 (1961).

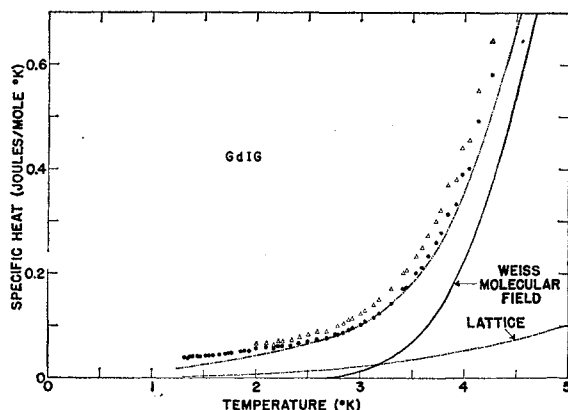


FIG. 3. The specific heat of GdIG between 1.3 and 4°K.  $\Delta$ , total specific heat;  $\bullet$ , magnetic specific heat. Dash-dotted line, calculated according to the spin-wave approximation with  $D=7.7\text{ cm}^{-1}$  and  $\hbar\omega_1=28.6\text{ cm}^{-1}$ . The curve according to the WMF model has been calculated for  $E_1=27.8\text{ cm}^{-1}$ .

Referring to Fig. 2, one sees that between 5 and 9°K the specific heat of LuIG is less than one would expect from Eq. (43), taking our values of  $D$  and  $\Theta$  whose determination below 5°K was rather convincing (see Fig. 1). We do not have an explanation for this anomalous behavior. Above 9°K, the specific heat of both LuIG and YIG becomes systematically larger than that given by Eq. (43) as extrapolated from helium temperatures. In view of our previous discussion (III D) we have attributed this excess specific heat to the lattice.

## 2. GdIG

In Figs. 3 and 4 we have plotted the total specific heat of GdIG and its decomposition into magnetic and lattice contributions as a function of temperature. Above 5°K, the data could be well represented using the Weiss molecular field approximation, Eq. (45b), with  $E_1=27.8\pm0.5\text{ cm}^{-1}$  which corresponds to an

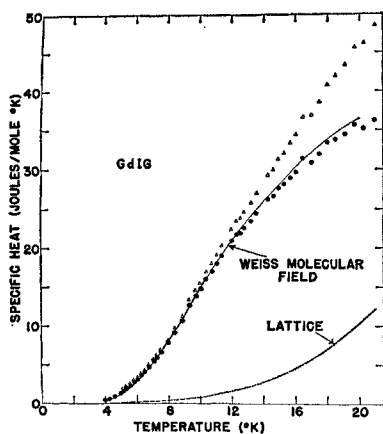


FIG. 4. The specific heat of GdIG between 4 and 21°K.  $\Delta$ , total specific heat;  $\bullet$ , magnetic specific heat. The WMF curve has been calculated for  $E_1=27.8\text{ cm}^{-1}$  and coincides practically with that calculated from the spin-wave approximation (not shown) up to about 16°K.

effective magnetic field of  $(3.00\pm0.06)\times10^5\text{ G}$ . In Fig. 3 we have also shown the theoretical curve for the magnetic specific heat using the spin-wave approximation Eq. (45a), taking  $\hbar\omega_1=28.6\pm0.5\text{ cm}^{-1}$  and  $D=7.7\pm0.5\text{ cm}^{-1}$ . Below 5°K, as one can see, the spin-wave treatment gives a much better agreement with experiment than the Weiss molecular field approximation.

Several points should be made. At temperatures above 5°K, the specific heat is relatively insensitive to the exact details of the spin-wave spectrum, so that the approximation of taking all the low optical modes to be degenerate seems very satisfactory. Above 15°K the lattice specific heat is somewhat uncertain, so that the small discrepancy between the calculated curve and the experimental data is not surprising. It seems to us that the suggestion<sup>20</sup> that there is a contribution to the specific heat from the variation of the zero-point energy resulting from the variation of the frequency spectrum is unjustified. Since we do not know the exact details of the spin-wave spectrum as determined by Dreyfus,<sup>20</sup> a direct comparison between his calculations and our experiments has not been made by us.

The values of  $E_1$  we have found can be compared with the result of magnetic measurements. Pauthenet,<sup>2</sup> using magnetization and susceptibility data at 20°K, found  $E_1$  to be  $24.9\text{ cm}^{-1}$ . From measurements of the susceptibility above the Curie point, Aléonard<sup>8</sup> deduced values of the interaction coefficients from which one finds  $E_1$  to be  $19.2\text{ cm}^{-1}$ . This value differs from the low-temperature determinations probably because the extrapolation of the interaction coefficients to low temperatures may be somewhat uncertain.

From Eq. (18) we see that one has approximately

$$D(\text{GdIG}) = D(\text{YIG}) \times S_{\text{tot}}(\text{YIG}) / S_{\text{tot}}(\text{GdIG}).$$

Taking  $D(\text{YIG})$  to be  $27\text{ cm}^{-1}$  from Table V,<sup>44-46</sup> we would expect  $D(\text{GdIG})$  to be approximately  $8.7\text{ cm}^{-1}$ . This is in reasonable agreement with the experiment. Below 2.5°K, there is an excess specific heat which cannot be accounted for by the spin-wave theory. This excess is approximately given by  $0.03/T^2\text{ J per M deg}$ . It may be due to unusually large nuclear splittings from polarization of  $s$  orbitals in the strong exchange field of the iron ions. Such an explanation would be rather surprising and this question will be investigated by specific heat measurements below 1°K and in magnetic fields.

## B. Non-S-State Ions

### 1. YbIG

In Figs. 5 and 6 we have plotted the total specific heat of YbIG and also  $(C_{\text{magn}} + C_{\text{nuc}})$  as a function

<sup>44</sup> H. J. McSkimin (private communication) found the transverse and longitudinal sound velocities at room temperature to be, respectively,  $V_t=3.87\times10^5\text{ cm/sec}$  and  $V_l=7.17\times10^5\text{ cm/sec}$ .

<sup>45</sup> E. H. Turner, Phys. Rev. Letters **5**, 100 (1960).

<sup>46</sup> R. C. LeCraw and L. R. Walker, J. Appl. Phys. **32**, 167S (1961).

of temperature between 1.3 and 20.5°K. Using the one-ion approximation Eq. (46), we have fitted the experimental values of the magnetic and the nuclear specific heat to the formula

$$6R \left( \frac{\bar{E}_1}{k_B T} \right)^2 \frac{e^{-\bar{E}_1/k_B T}}{(1+e^{-\bar{E}_1/k_B T})^2} + \frac{0.0158}{T^2} \frac{J}{\text{mole deg}}. \quad (47)$$

It should be noted that we were able to fit the experimental data assuming  $\bar{E} = E_1 = E_1'$ , i.e., that both sites had the same splitting. The value of  $\bar{E}_1$  which gave the best fit above 5°K was  $25.0 \pm 0.5 \text{ cm}^{-1}$ , corresponding to an effective magnetic field of about  $(1.55 \pm 0.03) \times 10^5 \text{ G}$ . It was not possible to determine unambiguously  $E_1$  and  $E_1'$  separately since the specific heat is not sensitive to small differences in these parameters providing that the average splitting is held constant. We concluded, however, that the two splittings did not differ by more than 15%. Analysis of the specific heat data showed that there were no higher excited electronic energy levels below say,  $75 \text{ cm}^{-1}$ . As mentioned before, the lowest doublet of  $\text{Yb}^{3+}$  in  $\text{YbIG}$  is separated from the

TABLE VI. Values of the splitting of the lowest doublet of  $\text{Yb}^{3+}$  in  $\text{YbIG}$ , in  $\text{cm}^{-1}$ .

Source	$E_1$	$E_1'$	$\bar{E}_1$
Specific heat (4–20°K)	...	...	25.0
Magnetization <sup>a</sup> (2.2–100°K)	...	...	25.5
Infrared absorption <sup>b</sup> (1.5°K)	23.4	26.4	24.9
Optical absorption <sup>c</sup> (77°K)	22.1	25.3	23.7
Susceptibility <sup>d</sup> (550–1450°K)	...	...	108.0
Estimated from $\text{GdIG}$ using Eq. (37)	...	...	11.9

<sup>a</sup> See reference 2.  
<sup>b</sup> See reference 47.

<sup>c</sup> See reference 48.  
<sup>d</sup> See reference 3.

excited states by an energy of the order of  $600 \text{ cm}^{-1}$  and thus does not contribute to the specific heat below  $20^\circ\text{K}$ .

In the region above  $10^\circ\text{K}$ , the experimental curve lies below the theoretical one, possibly as a result of the uncertainty in the lattice specific heat. Below  $4^\circ\text{K}$ , the specific heat becomes larger than what one would expect on the basis of the WMF model. Sievers and Tinkham<sup>47</sup> have determined directly the energy levels of the two sites by infrared absorption. Substituting their values below  $20^\circ\text{K}$ ,  $E_1 = 23.4 \text{ cm}^{-1}$  and  $E_1' = 26.4 \text{ cm}^{-1}$ , into Eq. (46) one finds a somewhat better fit with the experimental results below  $5^\circ\text{K}$  than our average value of  $25.0 \text{ cm}^{-1}$ . However, even with these values, the WMF approximation is far from sufficient to account for the specific heat below  $4^\circ\text{K}$ . This specific heat is probably due to the presence of the exchange mode  $\omega_2$  whose characteristic energy for  $\mathbf{k}=0$  is roughly  $\frac{3}{2}\bar{\omega}_1$  as given by Eq. (24). Tinkham<sup>6</sup> has made more accurate calculations and has found that for  $\mathbf{k}=0$  this

<sup>47</sup> A. J. Sievers, III, and M. Tinkham, Phys. Rev. **124**, 321 (1961).

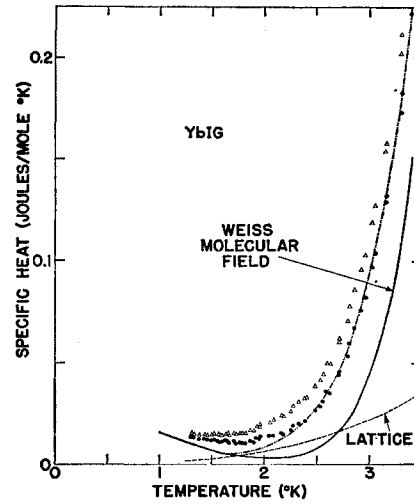


Fig. 5. Specific heat of  $\text{YbIG}$  between 1.3 and  $3^\circ\text{K}$ .  $\Delta$ , total specific heat;  $\bullet$ ,  $C_{\text{magn}} + C_{\text{nuc}}$ . The WMF curve is calculated from Eq. (47) with  $\bar{E}_1 = 25 \text{ cm}^{-1}$ . Dash-dotted line, curve calculated according to the spin-wave approximation with  $\hbar\omega_2 = 17.4 \text{ cm}^{-1}$  and  $\hbar\omega_1 = 26.0 \text{ cm}^{-1}$ .  $C_{\text{nuc}}$  is taken from Table III.

mode should have a characteristic energy of about  $14 \text{ cm}^{-1}$  at temperatures below  $10^\circ\text{K}$ , which is well confirmed by his experiment.<sup>47</sup> He has predicted that the average frequency of this mode as observed by specific heat measurements should practically coincide with that of the other low optical modes. However, the large specific heat between 2 and  $4^\circ\text{K}$  seems to indicate that the average frequency is well below that of the others. Our results can be well fitted by taking the average energy  $\hbar\omega_2$  to be  $17.4 \pm 0.8 \text{ cm}^{-1}$  and  $\hbar\omega_1 = 26.0 \pm 0.5 \text{ cm}^{-1}$  (see Fig. 5).

Our value of  $E_1$  can be compared with those deduced from other experiments given in Table VI. Using Aléonard's values of the interaction coefficients  $n_{ij}$  as

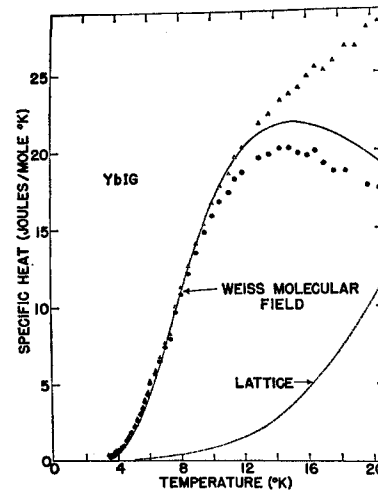


Fig. 6. Specific heat of  $\text{YbIG}$  between 3 and  $21^\circ\text{K}$ .  $\Delta$  = total specific heat;  $\bullet$  =  $C_{\text{magn}}$ . The WMF curve is calculated from Eq. (47) with  $E_1 = 25.0 \text{ cm}^{-1}$ .

deduced from susceptibility measurements above the Curie point,<sup>3</sup> one finds that  $E_1 = 108 \text{ cm}^{-1}$ . The large error in this value may result from the fact that the magnetic interactions determine how much  $\chi(\text{YbIG}) - \chi(\text{YIG})$  differs from the free-ion susceptibility of the  $\text{Yb}^{3+}$  ions. Since these two quantities differ by only 15%, very precise measurements of the susceptibility are needed to determine  $E_1$ . Assuming  $J_{ca}$  and  $J_{cd}$  to be the same for YbIG as for GdIG one finds, substituting the experimental determined value of  $E_1(\text{GdIG})$  into Eq. (37), that  $E_1(\text{YbIG})$  should be about  $12 \text{ cm}^{-1}$ . Thus we conclude that the iron-rare-earth exchange integrals are about twice as large in YbIG as in GdIG. Pauthenet<sup>2</sup> has plotted  $n' = n(L+2S)/(2S)$  vs the atomic number of the rare earth included in the iron garnet, where  $n$  is proportional to the exchange field acting on the rare earth ions. He finds that  $n'$  (and hence the iron-rare earth exchange integrals) decreases as one goes from GdIG towards YbIG. It is therefore quite anomalous that the exchange integrals are so large for YbIG. As Wickersheim has found,<sup>48</sup> the exchange field is highly anisotropic. As a result, the difference in the splitting of the two sites is much larger than one would expect from the anisotropy of the  $g$  values [See Eq. (37)].

## 2. HoIG and TbIG

For these garnets the nuclear splittings were quite large, so that it was necessary to use the expression (41a) for the specific heat. Fortunately both holmium and terbium have only one stable isotope, so that it is not necessary to average over isotopes. We shall neglect the possibility that the two inequivalent sites might have somewhat different nuclear splittings since specific heat data above  $1^\circ\text{K}$  could not resolve small differences in the splittings. In Figs. 7 and 8 we have plotted the total specific heat of HoIG between 1.6 and  $20^\circ\text{K}$ . Below  $4^\circ\text{K}$  the contribution from the nuclear spins becomes dominant. As can be seen, good agreement between the calculated and experimental values

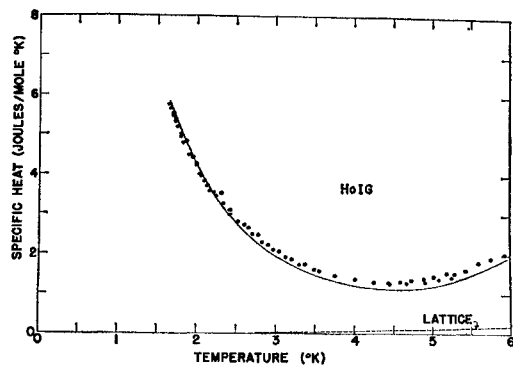


FIG. 7. Specific heat of HoIG between 1.5 and  $6^\circ\text{K}$ .  $\bullet = C_{\text{nuc}} + C_{\text{magn}}$ . The curve is that calculated according to the WMF model using Eqs. (41a), (46), and (48) with  $\Delta = 0.181 \text{ cm}^{-1}$ .

<sup>48</sup> K. A. Wickersheim, Phys. Rev. **122**, 1376 (1961).

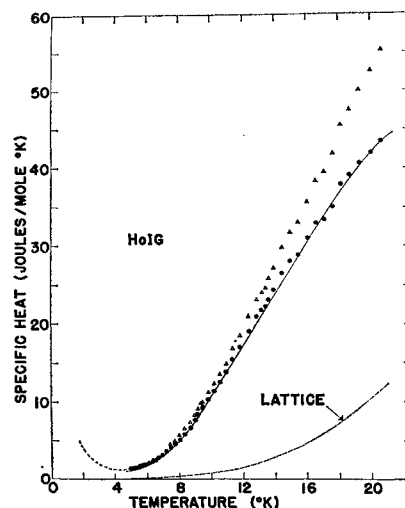


FIG. 8. Specific heat of HoIG between 5 and  $21^\circ\text{K}$ .  $\Delta$  = total specific heat;  $\bullet = C_{\text{nuc}} + C_{\text{magn}}$ . The drawn curve is calculated from the WMF approximation using Eqs. (41a), (46), and (48), and  $\Delta = 0.181 \text{ cm}^{-1}$ .

of the specific heat was obtained by taking the nuclear splitting to be  $0.181 \pm 0.006 \text{ cm}^{-1}$  for both inequivalent sites.

Above  $6^\circ\text{K}$  the nuclear specific heat becomes unimportant. Comparing the experimental values of the magnetic specific heat with specially tabulated functions, we found good agreement by assuming that the energy level schemes of the two inequivalent sites were the same. The values of  $E_i$  and  $g_i$ , the energy and degeneracy of the  $i$ th excited energy level, which gave the best fit were

$$\begin{aligned} E_1 &= 32.4 \pm 0.6 \text{ cm}^{-1}, & g_1 &= 1, \\ E_2 &= 69 \pm 3 \text{ cm}^{-1}, & g_2 &= 3. \end{aligned} \quad (48)$$

The determination of the high energy levels was not conclusive, as a reasonable fit could also be obtained

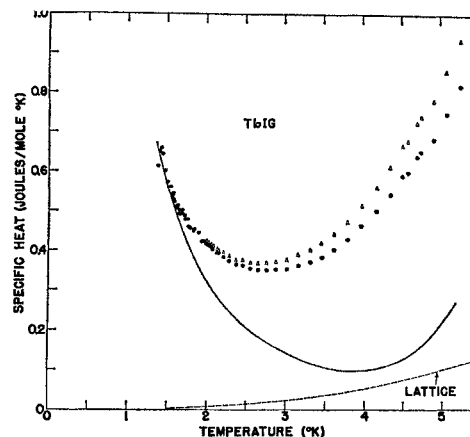


FIG. 9. Specific heat of TbIG between 1.3 and  $5^\circ\text{K}$ .  $\Delta$  = total specific heat;  $\bullet = C_{\text{magn}} + C_{\text{nuc}}$ . The drawn curve is calculated from the WMF model using Eqs. (41a), (46), and (50) with  $\Delta = 0.10 \text{ cm}^{-1}$ .

taking

$$E_2 = 71 \pm 3 \text{ cm}^{-1}, \quad g_2 = 4. \quad (49)$$

We can now compare the value of the nuclear splitting with values predicted from data on the nuclear splitting in the ethylsulphate.<sup>38</sup> In Table III we predicted the nuclear splitting to be  $0.139 \text{ cm}^{-1}$  as contrasted to the experimental value of  $0.181 \text{ cm}^{-1}$ . As we have remarked, our estimates can be too low by the order of 20% because of the canting of the moments. Considering this, our experimental value is quite reasonable.

For TbIG we were not able to fit the experimental values convincingly. It was assumed that at  $1.4^\circ\text{K}$  all the specific heat was due to nuclear interactions. Assuming the nuclear splitting was the same for both inequivalent sites, we found that  $\Delta = 0.10 \pm 0.01 \text{ cm}^{-1}$ . As can be seen in Fig. 9, the calculated and experimental values of  $(C_{\text{magn}} + C_{\text{nuc}})$  start to diverge above  $2^\circ\text{K}$ . This discrepancy can not be avoided by choosing different electronic energy level splittings, since the experimental data above about  $6^\circ\text{K}$  would not permit energy smaller level splittings. Only the positions of the first excited levels could be determined. For the two sites we found

$$\begin{aligned} E_1 &= 36 \pm 4 \text{ cm}^{-1} \text{ for site 1,} \\ E_2 &= 50 \pm 6 \text{ cm}^{-1} \text{ for site 2.} \end{aligned} \quad (50)$$

As can be seen in Figs. 9 and 10, the fit is poor between about 2 and  $10^\circ\text{K}$ , and consequently our determination of the energy levels must be considered somewhat uncertain. In this temperature region the lattice specific heat can not be a source of error, so this discrepancy is somewhat surprising. We were unable to secure a reasonable fit even by assuming that, as for YbIG, this excess heat was due to an exchange mode lying well below the other modes. Since the specific heat at  $20^\circ\text{K}$  is so small, one concludes that the higher excited energy levels lie probably more than  $80 \text{ cm}^{-1}$

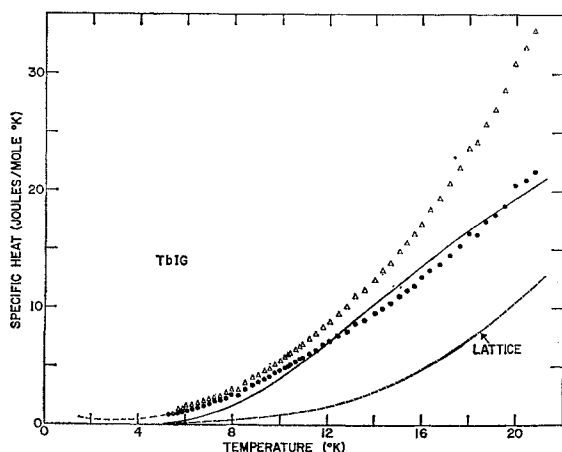


FIG. 10. Specific heat of TbIG between 5 and  $21^\circ\text{K}$ .  $\Delta$  = total specific heat;  $\bullet$  =  $C_{\text{nuc}} + C_{\text{magn}}$ . The drawn curve is calculated from the WMF approximation using Eqs. (41a), (46), and (50) with  $\Delta = 0.10 \text{ cm}^{-1}$ .

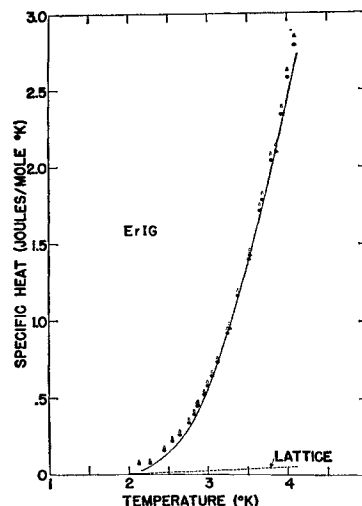


FIG. 11. Specific heat of ErIG between 2 and  $4^\circ\text{K}$ .  $\Delta$  = total specific heat;  $\bullet$  =  $C_{\text{nuc}} + C_{\text{magn}}$ . The drawn curve is calculated from the WMF model using Eqs. (46) and (51).

above the ground state. Again we can compare the nuclear splitting we have found with that one would expect from paramagnetic resonance data obtained in the ethylsulphate. In Table III we predicted the nuclear splitting to be about  $0.084 \text{ cm}^{-1}$  as contrasted to the experimental value of  $0.10 \text{ cm}^{-1}$ . The fact that our estimate is too low may again be due to the canting of the electronic moments.

### 3. ErIG and DyIG

In Figs. 11 and 12 we have plotted the specific heat of ErIG as a function of temperature between 2.1 and  $21^\circ\text{K}$ . The nuclear specific heat, calculated in

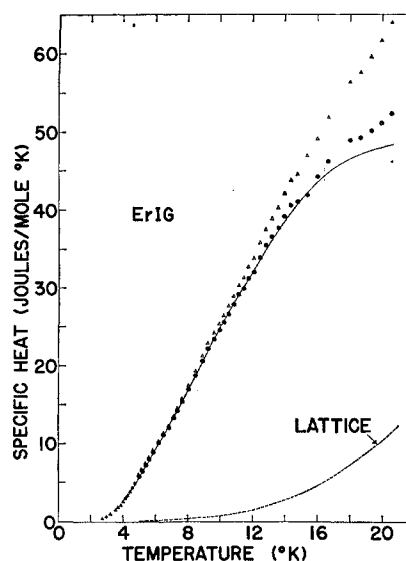


FIG. 12. Specific heat of ErIG between 4 and  $21^\circ\text{K}$ .  $\Delta$  = total specific heat;  $\bullet$  =  $C_{\text{magn}}$ . The drawn curve is calculated from the WMF model using Eqs. (46) and (51).

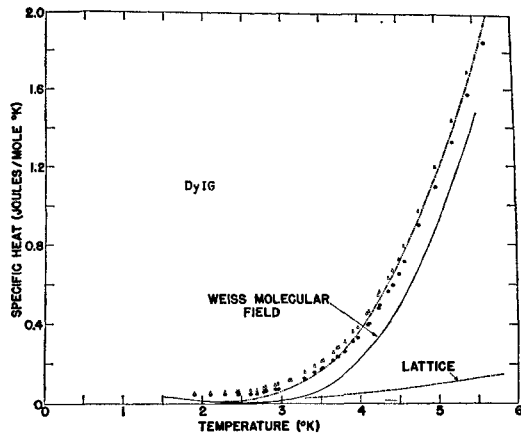


FIG. 13. Specific heat of DyIG between 2 and 6°K.  $\Delta$  = total specific heat;  $\bullet$  =  $C_{\text{magn}} + C_{\text{nuc}}$ . The drawn curve is calculated from the WMF approximation using Eqs. (46) and (52) and Table III. Dash-dotted line, calculated in the spin-wave approximation taking  $\hbar\omega_2 = 18.8 \text{ cm}^{-1}$ , five modes  $\hbar\omega_1 = 24.7 \text{ cm}^{-1}$ , five modes  $\hbar\omega_1' = 40.1 \text{ cm}^{-1}$ , and one mode  $\hbar\omega_1'' = 32 \text{ cm}^{-1}$ .

Table III made only a small contribution, as expected. It was found that the experimental results could well be accounted for by using the WMF approximation with the following energy level schemes

$$\text{and } \left. \begin{array}{ll} E_1 = 16.8 \pm 0.5 \text{ cm}^{-1}, & g_1 = 1 \\ E_2 = 50 \pm 2 \text{ cm}^{-1}, & g_2 = 3 \end{array} \right\} \text{site 1} \quad (51)$$

$$\left. \begin{array}{ll} E_1' = 24.6 \pm 0.7 \text{ cm}^{-1}, & g_1' = 1 \\ E_2' = 50 \pm 2 \text{ cm}^{-1}, & g_2' = 3 \end{array} \right\} \text{site 2}.$$

As can be seen in the figures, the agreement between the experimental values of the magnetic specific heat and that resulting from the above energy level schemes is remarkably good down to 3°K. Only the energy and degeneracy of the first excited state  $E_1$  and  $E_1'$  can be unambiguously determined from the experimental data, so that the values of  $E_2$  and  $E_2'$  should be con-

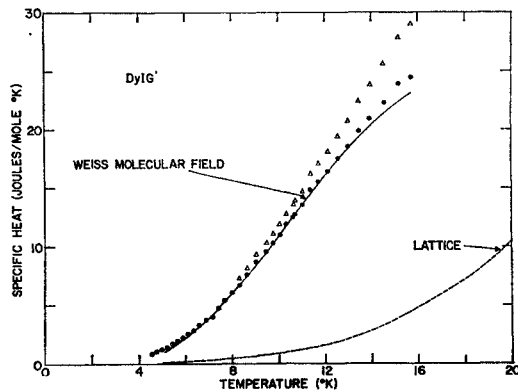


FIG. 14. Specific heat of DyIG between 5 and 16°K.  $\Delta$  = total specific heat;  $\bullet$  =  $C_{\text{magn}} + C_{\text{nuc}}$ . The drawn curve is calculated according to the WMF approximation using Eqs. (46) and (52).

sidered to be the average energy of several excited states.

Sievers and Tinkham<sup>6</sup> have carried out infrared absorption measurements and find absorptions at 18.2 and 21.6  $\text{cm}^{-1}$  which they attribute to the exchange splittings of the two inequivalent sites, and also at 10  $\text{cm}^{-1}$  due to the presence of the exchange mode  $\omega_2$ . They also find several higher levels which probably give an excess specific heat equivalent to our group of levels near 50  $\text{cm}^{-1}$ . The excess specific heat below 3°K (see Fig. 11) can best be accounted for by using the spin-wave approximation and taking the average energy of the exchange mode to be about 15  $\text{cm}^{-1}$ . With this model, the specific heat results could be well fitted taking the energies of the two inequivalent sites to be, respectively, 18.3 and 22.7  $\text{cm}^{-1}$ , in fair agreement with Tinkham's values.<sup>47</sup>

In Figs. 13 and 14 we have plotted the specific heat of DyIG as a function of temperature between 1.9 and 16°K. The nuclear specific heat was estimated in Table III and was important only at the lowest temperatures. In order to fit the experimental values of the magnetic specific heat, it was again necessary to take different energy level schemes for the two inequivalent sites. We found, using the WMF approximation,

$$\text{and } \left. \begin{array}{ll} E_1 = 24.7 \pm 0.7 \text{ cm}^{-1}, & g_1 = 1 \\ E_2 = 60 \pm 3 \text{ cm}^{-1}, & g_2 = 1 \end{array} \right\} \text{site 1} \quad (52)$$

$$\left. \begin{array}{ll} E_1' = 40.1 \pm 1.0 \text{ cm}^{-1}, & g_1' = 1 \\ E_2' = 65 \pm 3 \text{ cm}^{-1}, & g_2' = 1 \end{array} \right\} \text{site 2}.$$

As can be seen, the specific heat calculated from these energy levels fits the experimental values of the magnetic specific heat satisfactorily above 4.5°K. Below this temperature there is again a large excess specific heat

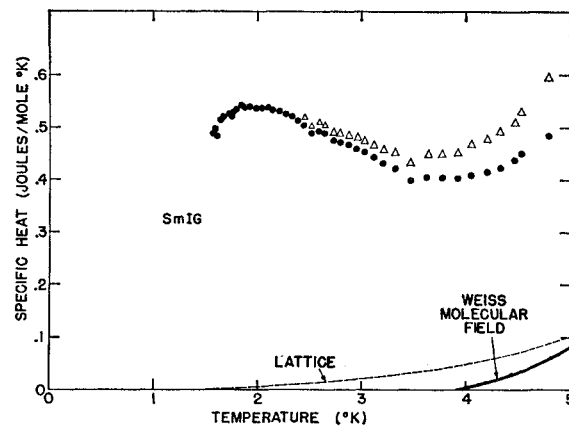


FIG. 15. Specific heat of SmIG between 1.6 and 5°K.  $\Delta$  = total specific heat;  $\bullet$  =  $C_{\text{magn}} + C_{\text{nuc}}$ . The curve is calculated from the WMF approximation using Eqs. (46) and (53). The nuclear specific heat was estimated to be negligible.



which could be attributed to the presence of a low-lying optical mode (in the spin-wave approximation) whose average characteristic energy was  $18.8 \pm 0.8 \text{ cm}^{-1}$ , (see Fig. 13). Again for DyIG the position of the energy levels above the first excited one is somewhat ambiguous, as good agreement with the experimental data could also be obtained taking  $E_2 = E_2' = 70 \pm 3 \text{ cm}^{-1}$  and  $g_2 = g_2' = 2$ . The fact that the lattice specific heat is not small in comparison to the magnetic contribution above about  $12^\circ\text{K}$  also introduces some uncertainty into the determination of the energy level scheme.

#### 4. SmIG

The specific heat of SmIG is plotted in Figs. 15 and 16 as a function of temperature between 1.6 and  $20^\circ\text{K}$ . Above about  $8^\circ\text{K}$  the magnetic specific heat could be approximated by the specific heat resulting from the energy level schemes

$$\begin{aligned} E_1 &= 36.1 \pm 3 \text{ cm}^{-1}, & g_1 &= 1 \text{ for site 1,} \\ E_1' &= 70 \pm 10 \text{ cm}^{-1}, & g_1' &= 1 \text{ for site 2.} \end{aligned} \quad (53)$$

There is no evidence of any other levels below, say,  $100 \text{ cm}^{-1}$ . Above  $15^\circ\text{K}$  the lattice specific heat became comparable to the magnetic contribution, so that the determination of the energy levels, especially for site 2, was somewhat uncertain.

Below  $4^\circ\text{K}$  the specific heat increases, passing through a maximum at  $1.95^\circ\text{K}$ . This type of behavior cannot result from the nuclear or electronic splittings because the height of this maximum is much too small. In addition, in analogy with samarium ethylsulfate,<sup>26</sup> one expects a rather small nuclear splitting giving a negligible specific heat tail above  $1^\circ\text{K}$ . The magnetic specific heat below  $3.5^\circ\text{K}$  can be very well fitted if one

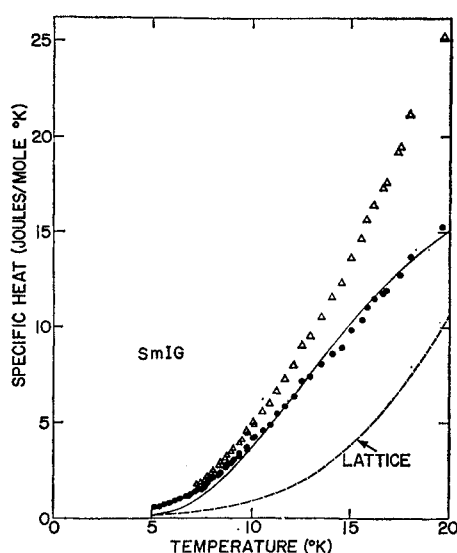


FIG. 16. Specific heat of SmIG between 5 and  $20^\circ\text{K}$ .  $\Delta$  = total specific heat;  $\bullet$  =  $C_{\text{magn}}$ . The curve is calculated from the WMF approximation using Eqs. (46) and (53).

assumes that the 2 or 3% impurity in the sample has a Schottky anomaly arising from two energy levels whose separation is about  $3.8 \text{ cm}^{-1}$ . Measurements on another sample of SmIG will be undertaken to see whether this is the correct explanation for this anomaly. It is rather strange, however, that none of the other samples exhibited this behavior, although they probably also contained some traces of oxides.

The infrared absorption spectrum of SmIG was investigated by Sievers and Tinkham<sup>6</sup> who found four absorption lines at 20, 33.5, 52, and  $83 \text{ cm}^{-1}$  at  $2^\circ\text{K}$ . They have not been able so far to relate their absorption spectrum to the energy levels estimated from calorimetry.

#### C. Conclusion

Figure 17 shows the energy level diagrams of the rare earth ions in the iron garnets using the WMF approximation. It is estimated that the temperature variation of these levels below  $20^\circ\text{K}$  is too small to affect the specific heat. Above this temperature, the WMF will diminish progressively with the magnetization of the  $a$ ,  $d$ , and  $c$  sublattices. Except for TbIG and SmIG below  $8^\circ\text{K}$ , the specific heat as calculated from these energy levels agrees rather well with the observed specific heat down to about  $3\text{--}4^\circ\text{K}$ . Even though the exact details of the energy level schemes may be ambiguous in certain cases, several general facts are evident. First of all, the exchange splitting of the rare-earth ion in the garnets is generally different for the two inequivalent sites, which implies that the local symmetry of the sites is noncubic. The splittings of the two sites can differ by a factor as large as about 2, which can be expected from the large anisotropy of the  $g$  values of the ground doublet.<sup>39</sup> Secondly, we also find that there are energy levels which lie rather close to the first-excited level and hence we conclude that the crystalline field splittings are of the same order of magnitude as the exchange splittings. In qualitative

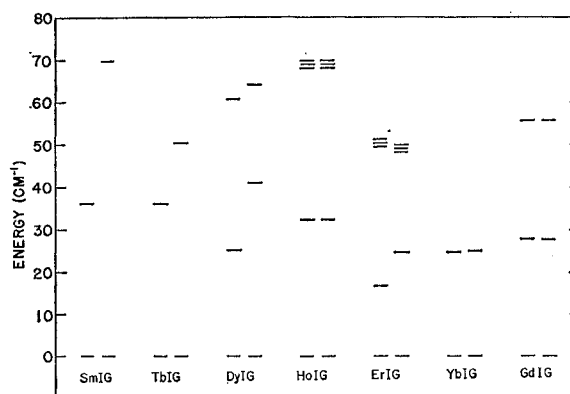


FIG. 17. Position of the electronic energy levels of the two inequivalent rare earth ions in the iron garnets, according to the WMF approximation for temperatures below  $20^\circ\text{K}$ . For GdIG there are eight equally spaced levels, of which only the three lowest are shown here.

agreement with these conclusions, the size of the crystalline field splittings in the gallium and aluminum garnets has been shown<sup>39</sup> to be of the same order of magnitude as the exchange splittings in the iron garnets. Since in most cases the wave functions of the rare earth ions were unknown, it was impossible to make comparisons with magnetic measurements. In addition, since the exchange field was often comparable to the crystalline field, no conclusions about the size of the exchange integral could be drawn by comparing the splittings to those of GdIG.

Below about 4°K, the measured magnetic specific heat was always appreciably larger than that calculated from the WMF approximation. Using the spin-wave model, one can explain this excess satisfactorily by attributing it to the excitation of the acoustical mode or the exchange mode  $\omega_2$ . In view of our results, we conclude that the WMF approximation is valid for  $k_B T \gtrsim E_1/6$  where  $E_1$  is the exchange splitting. On the other hand, for  $k_B T \lesssim E_1/3$  the spin-wave approximation is valid. In the overlapping region, the two models fit our data equally well, as expected.

Although most of our results can be understood within the framework of existing theoretical models, the low-temperature behavior of several garnets require further theoretical and experimental study.

(1) On the one hand,  $\text{Sm}^{3+}$  in SmIG shows large exchange splittings as deduced from specific heat measurements, and on the other hand it fails to influence appreciably the magnetization.<sup>2</sup>

(2) The specific heat of TbIG between 1.4 and 6°K can not be analyzed satisfactorily in terms of either of the above mentioned approximations.

(3) The specific heat of GdIG below 2.5°K is systematically larger than expected from spin-wave theory and requires further clarification.

Extension of the present program to other garnet samples and still lower temperature regions is being undertaken presently.

#### ACKNOWLEDGMENTS

The experimental part of this work and most of the calculations were performed at Harvard University and were supported by a contract Nonr-1866(26) and AF 19(604). The work was continued at Duke University where it was supported by the contract Nonr 1181(12), the grant DA-ORD-4, and a grant from the Alfred P. Sloan Foundation.

We are most indebted to Carlos Quadros and Mrs. L. Lin at Harvard for the preparation of the samples, to Dr.

J. E. Kunzler for providing the YIG sample and to Professor Frondel for analyzing the SmIG specimen. We wish to acknowledge stimulating discussions on our results with Professor R. V. Jones, Professor J. H. Van Vleck, and Dr. G. Seidel. We are indebted to Professor M. Tinkham for communicating to us some of his infrared absorption results before publication. We also thank the staff of the M.I.T. computation laboratory for help in tabulating specific heat functions.

#### APPENDIX

##### The Acoustic Mode for Garnets where the Rare Earth Ion is not in an *S* State

When the rare-earth ion is not in an *S* state, and providing the temperature is sufficiently low, the effective anisotropy field is much larger than the demagnetizing field. In this case the magnetization will lie along an easy direction, and consequently one can show<sup>14</sup> that the specific heat of the acoustic mode will be less than  $0.235(k_B T/D)^3 \exp(-g\beta H_{\text{anis}}/k_B T)$ . Here  $H_{\text{anis}} = 4KV/3M$ , since the easy axis coincides with a  $[111]$  direction. In discussing the effect of the crystalline field on *D* we need only consider how  $S_{\text{tot}}$  is modified, since the exchange integrals involving the rare earth ion are much smaller than those which involve only iron ions. Insofar as the crystalline field splittings are much larger than those caused by the exchange field, one needs only consider matrix elements of the exchange Hamiltonian within the lowest manifold of crystalline field states. Although this condition is not well fulfilled for several of the garnets, the following argument should still have qualitative validity. In writing the spin Hamiltonian one replaces  $(L+2S)$  by  $g_{\text{eff}}S_{\text{eff}}$ , where  $g_{\text{eff}}$  is the effective *g* tensor and  $S_{\text{eff}}$  is the effective spin, which is such that  $2S_{\text{eff}}+1$  is equal to the degeneracy of the manifold.  $S_{\text{eff}}$  obeys the same commutation relations as a real spin of  $S_{\text{eff}}$ ,<sup>40</sup> and consequently one sees that in the expression for  $S_{\text{tot}}$  one should always use effective spin values. Since the crystalline field is noncubic, the effective spin appropriate to the *c* sublattice is either  $\frac{1}{2}$  or 1, which gives  $S_{\text{tot}}$  equal to 8 or 4, respectively. Using Eq. (18) we see that *D* for garnets whose rare earth ions are not in *S* states is thus larger than *D*(YIG) by at least a factor of 2.5. Thus the specific heat of the acoustic mode will be greatly reduced in comparison to that of YIG, especially in the temperature region where the specific heat of the optical modes is small and might otherwise permit its observation.

<sup>40</sup> J. H. Van Vleck, Phys. Rev. **123**, 58 (1961).